Role of ER exit sites in GRASP-mediated unconventional secretion pathway

He Piao

Department of Medical Science

The Graduate School, Yonsei University

Role of ER exit sites in GRASP-mediated unconventional secretion pathway

Directed by Professor Min Goo Lee

The Doctoral Dissertation
submitted to the Department of Medical Science,
the Graduate School of Yonsei University
in partial fulfillment of the requirements for the degree of
Doctor of Philosophy

He Piao

December 2016

This certifies that the Doctoral Dissertation of He Piao is approved.

Thesis Supervisor: Min Goo Lee

Thesis Committee Member #1: Soo Han Bae

Thesis Committee Member #2: Joo Young Kim

Thesis Committee Member #3: Wan Namkung

Thesis Committee Member #4: Ki Taek Nam

The Graduate School

Yonsei University

December 2016

ACKNOWLEDGEMENTS

석박사 통합과정 동안 저에게 도움을 주시고 힘이 되어주신 많은 분들 덕분에 학위 과정을 무사히 마칠 수 있었습니다. 먼저 부족한 저에게 약리학교실에서 공부할 수 있는 기회를 주셨고, 정성과 지혜로 학문에 대한 흥미를 키워주시고 또한 인생의 본보기가 되어주신 지도교수 이민구 교수님께 진심으로 감사 드립니다. 저에게 약리학 연구의 길을 열어주시고 진심 어린 조언과 격려를 주셨던 진정애 교수님께 감사 드립니다. 연구에 입문하고 성장할 수 있도록 가르쳐주시고 또한 학위논문 심사해주신 김주영 교수님께 진심으로 감사 드립니다. 연구와 진로 결정에 있어서 주옥 같은 조언을 해주시고 학위과정 마무리 단계에서 도움을 주신 랩 선배님 지헌영 교수님께 감사 드립니다. 바쁘신 와중에 저의 학위 논문을 검토해주시고, 심사해주신 배수한 교수님, 남궁완 교수님, 남기택 교수님께 감사 드립니다. 또한 약리학을 전공 하게 허락해주시고 본받아 배울 수 있게 해주신 김경환 명예교수님, 안영수 명예교수님, 김동구 교수님, 박경수 교수님, 김철훈 교수님, 김형범 교수님께도 감사 드립니다.

학위 과정 동안 함께 생활 하면서 많은 도움을 주신 민선자 선생님, 임종수 선생님을 비롯한 약리학 교실 선생님들께도 감사 드립니다. 학위과정의 시작과 끝에서 연구하는 사고방식을 잘 잡을 수 있도록 진심 어린 조언을 해주신 박현우 선생님께 감사 드립니다. 그리고 제가 랩에 처음 들어왔을 때 사수로서 여러 가지 많은 것을 가르쳐주신 정우영 선생님께 감사 드립니다. 입학 때부터 졸업할 때까지 따듯한 마음으로 챙겨주신 형순 오라버님께 감사 드립니다. 그리고 늘 한결 같이 랩 생활을 잘 할 수 있도록 도와주시는 우리 랩 메니져 정남 언니, 여러모로 저를 챙겨주신 다정한 신혜 언니, 옆에서 지속적인 동기부여가 됐고 같이 졸업하는 익현 오빠, 랩에서 고민을 가장 많이 나눴던 짝꿍 수민 언니, 격려를 많이 해주시고 비전을 보여주신 한상 오빠, 그리고 동고동락하는

우리 랩 김연정 선생님, 신동훈 선생님, 엄소원 선생님, 김지윤 선생님, 운이, 경지, 이준석 선생님, 영익이, 세영이; 졸업하셨지만 긴 시간 동안 함께 공부하고 좋은 팁들을 가르쳐 주셨던 진세 오빠, 소원 오빠, 준희 언니, 은석 오빠, 유일한 입학동기 정우 오빠, 혜민 언니, 모두 감사합니다. 또한 함께 공부하면서 친분을 쌓아온 지혜 언니, 태훈이, 동희 에게도 고맙다고 말하고 싶습니다. 연구실 인턴으로 우리 랩에서 지냈지만 배울 점이 많고 또한 기쁨과 고민을 나누는 소중한 벗이 되어준 성호, 민지 에게도 진심으로 감사함을 전하고 싶습니다. 옆 연구실에서 먼저 제게 다가와 주신 친절한 한수정 언니께도 감사 드립니다. 논문의 완성에 있어서 실험적으로 도움을 주신 권희석 선생님, 김미정 선생님 그리고 모식도 그림편집을 도와주신 장동수 선생님께도 감사 드립니다. 앞으로 여러 고마운 분들께 저의 힘이 닿는 만큼 도움을 드리고 싶습니다.

지금의 모습으로 성장 할 수 있도록 저를 정성과 사랑으로 키워주시고, 항상 믿어주시고 지지해주시고 또 걱정해주시는 세상에서 가장 소중한 우리 아빠, 엄마: 감사하고 사랑합니다. 앞으로도 부모님께 더욱 자랑스러운 딸이 될 수 있도록 열심히 살아가겠습니다. 저를 어릴 때부터 정말 예뻐 해주시고 키워주셨던, 그리고 제가 꼭 박사가 되기를 소망하셨던 우리 할머니, 외할머니께도 하늘나라를 향해 감사와 사랑하는 마음을 올립니다. 항상 저를 예뻐 해주시고 자랑스러워 하시는 우리 할아버지, 우리 가족들 모두 진심으로 감사 드립니다. 마지막으로 미래에 제 인생의 동반자가 되어줄 사람에게도 저의 열정과 노력이 고스란히 담긴 박사학위논문을 감사와 사랑하는 마음으로 드리고 싶습니다.

2016.12.08

박학

TABLE OF CONTENTS

LIST OF FIGURES

LIST OF TABLES

Abstract

Role of ER exit sites in GRASP-mediated unconventional secretion pathway

He Piao

Department of Medical Science
The Graduate School, Yonsei University

(Directed by Professor Min Goo Lee)

Deletion of phenylalanine at position 508 of the transmembrane protein CFTR is the most common form of disease-causing CFTR mutation, results in protein misfolding and deficiency of expressing at the cell surface. It has been shown that ER-to-Golgi blockade or GRASP overexpression could activate ΔF508-CFTR to be rescued to the cell surface through a Golgi by-pass unconventional secretion pathway. However, it is entirely unknown how misfolded ΔF508-CFTR can exit the endoplasmic reticulum (ER) membrane. Here we show that Sec16A, the key regulator of ER exit sites (ERES) formation is involved in the initiation of unconventional secretion. We found that dysfunction of Sec16A abolished both conventional and unconventional secretion of CFTR but other COPII-related components did not. During the unconventional secretion, Sec16A associated with GRASP and synchronized its localization change with GRASP, indicating that Sec16A supported GRASP to assemble with ΔF508-CFTR at the ERES nearby the cell periphery. Moreover, IRE1α-mediated UPR was identified as an upstream regulator for Sec16A responding to ER stress associated with unconventional secretion. These findings highlight the novel function of Sec16A working as key regulator for ER stress associated unconventional secretion.

Key Words: CFTR, ER exit sites, Sec16A, GRASP, unconventional secretion, IRE1α

Role of ER exit sites in GRASP-mediated unconventional secretion pathway

He Piao

Department of Medical Science
The Graduate School, Yonsei University

(Directed by Professor Min Goo Lee)

I. INTRODUCTION

Cystic fibrosis transmembrane conductance regulator (CFTR) is a membrane associated, N-linked glycoprotein with anion channel activity which is encoded by the gene associated with cystic fibrosis.[1] The CFTR protein can exist as non-glycosylated, core-glycosylated and complex-glycosylated (fully mature) forms.[2] CFTR is a cyclic AMP (cAMP)-activated chloride and bicarbonate channel and the fully glycosylated mature CFTR can express in the plasma membrane (PM) of secretory epithelia in the airways, intestine, pancreas and exocrine glands.[3,4] Therefore, loss-of-function mutations in CFTR causes autosomal recessive diseases associated with cystic fibrosis (CF) and other human diseases including bronchiectasis and chronic pancreatitis.[5,6] The most common cystic fibrosis (CF)-causing CFTR mutation is a three base pair deletion resulting in loss of phenylalanine residue at the position 508 (ΔF508).[7] ΔF508-CFTR is an incompletely glycosylated mutation which has defect in its folding resulting in its retention in the endoplasmic reticulum (ER) and being targeted to ER-associated degradation (ERAD) pathway.[8] However, the core-glycosylated ΔF508-CFTR can also function as a chloride channel when its dysfunction was corrected and transported to the cell surface.[9]

What's interesting is the core-glycosylated ΔF508-CFTR or wild-type CFTR can travel to

the cell surface through a Golgi reassembly stacking protein (GRASP)-dependent Golgi-bypass manner,[10] which is known as unconventional protein secretion.[11] Upregulation of GRASPs alone or ER-to-Golgi blockade could rescue the core-glycosylated ΔF508-CFTR transport to the cell surface of eukaryotic cells. Moreover, it has been shown that GRASP55 overexpression could rescue the defects caused by ΔF508-CFTR mutation in murine CF model.[10] Nevertheless, the precise machinery that the core-glycosylated CFTR could be survived from ER retention and then exports from the ER has not been identified.

The Golgi matrix proteins GRASPs including GRASP65 and GRASP55 were firstly identified as Golgi stacking factors[12-14] and also regulate Golgi ribbon formation.[15] Previous research proposed that yeast and drosophila homologues of GRASPs, Grh1 and dGRASP respectively, are dispensable for organizing conventional ER-to-Golgi secretory pathway.[16,17] And GRASP65/55 were characterized as a negative regulator of exocytic transport.[18] However, GRASPs specifically associate with cargo molecules through their PDZ domains and relieve the misfolded proteins from ER and facilitate them travel through the Golgi-independent route to the cell surface.[10] Starvation induced unconventional secretion of AcbA, the homologue of Acyl coenzyme A (CoA) binding protein in *Dictyostelium discoideum*, also requires GRASP (Grh1) and autophagosome formation.[19,20] Additionally, biogenesis of these unconventional protein secretion compartments initiates from Grh1 (GRASP homologue in *Saccharomyces cereviae*) recruiting to unique membrane structures of ER.[21]

The export of secretory proteins from the endoplasmic reticulum (ER) is mediated by COPII-coated vesicles that bud from specific locations on the ER membrane named ER exit sites (ERES).[22] COPII assembly starts with the activation of the small GTPase Sar1[23] which is catalyzed by Sec12 and completes with sequential recruitment of the Sec23-24 dimer to form the inner layer and the later assembling of Sec13-31 dimer to compose the outer layer of the COPII coat.[24,25] Sec16 is a large peripheral membrane protein of ~240KDa tightly associated with ERES and is proposed to act as a scaffold for assembly of COPII by interacting with multiple COPII components Sec23, Sec24, Sec13, Sec31 as well as Sar1 GTPase [26,27] and mediates the biogenesis of the ERES.[28] Human Sec16 is encoded by two

orthologue genes including Sec16A and Sec16B and Sec16A can be seen as the primary orthologue as it is most similar to Sec16 (~240KDa, in size) of other species. The robust localization of Sec16A due to its high charged region and it localizes at the ERES independently of downstream COPII proteins.[29] As a key regulator of ERES and COPII vesicle biogenesis, Sec16A controls the number of ERES via an ERK-2 dependent manner.[30] In order to adapt to the cargo load increment in the ER lumen, ERES number increases together with Sec16A level. Interestingly, inositol-requiring enzyme 1 (IRE1) mediated unfolded protein response (UPR) was reported to regulate Sec16A for manipulating this adaptive response of ERES.[31] The UPR is triggered by ER stress sensors containing IRE1α, PERK, and ATF6.[32] Importantly, IRE1-mediated signaling also has been shown involved in the GRASP-mediated surface trafficking of ΔF508-CFTR.[10]

Results of the initial RNA interference (RNAi) screening of COPII-associated components showed that depletion of Sec16A reduced the unconventional secretion of wild-type CFTR and ΔF508-CFTR induced by ER-to-Golgi blockade but other COPII components did not. Then we examined the role of Sec16A in the unconventional secretion pathway and identified that Sec16A plays a critical role in GRASP-mediated and ER stress induced unconventional secretion of core-glycosylated ΔF508-CFTR. These results provide new insights into the scaffolding role of Sec16A in formation of unconventional secretory vesicles and in the initiation of misfolded proteins export from ER to start the Golgi-bypass travel. Our findings provide a novel insight that Sec16A plays as a common platform for both conventional and unconventional export of secretory proteins from the ER.

II. MATERIALS AND METHODS

1. Cell line and Cell culture, Plasmids, Transfection, gene silencing and chemicals

HEK293 cells and HeLa cells were maintained in Dulbecco's modified Eagle's medium (DMEM high glucose) containing 10% fetal bovine serum (FBS) and penicillin (50 IU/mL)/ streptomycin (50 μg/mL) (all from Invitrogen) in 5% CO_2 incubator at 37 °C. The mammalian expression plasmid Sec16A-Myc/DDK (plasmid # RC223625) was purchased from OriGene. The plasmids encoding human ΔF508-CFTR, Myc-GRASP55, HA-Arf1-Q71L, Myc-Sar1-T39N, extracellular tagged HA-CFTR and HA-ΔF508-CFTR were described previously.[10] cDNAs of no-tagged GRASP55 were subcloned into pCMV-SPORT6 vector and cDNA of GRASP55-Myc was subcloned into pCMV-myc vector. Flag-tagged dynamin2-K44A was generated by a PCR-based site directed mutagenesis after constructing pcDNA3.1(+)-hDynamin2 using a cDNA fragment amplified from HEK293 cells (gene ID:1785, 2613 bp). pEYFP-ER plasmid was purchased from BD Biosciences (San Jose, CA, USA). Plasmid DNA transfection into HEK293 cells or HeLa cells were performed using TransIT-X2 Dynamic Delivery System (Mirus Bio LLC). siRNA duplexes were transfected into the HEK293 cells using Lipofectamine 2000 reagent (Invitrogen) according to the manufacturer's protocol. ON-TARGETplus human Sec16B-siRNA, Sec23A-siRNA, Sec23B-siRNA, Sec24A-siRNA, Sec24B-siRNA, Sec24C-siRNA, Sec24D-siRNA, Sec31B-siRNA and IRE1α-siRNA were purchased commercially (SMARTpool; Dharmacon, Lafayette, CO, USA). Synthesis of the following double strand siRNAs: siRNA against human Sec16A (targeting the sequence CCAGGTGTTTAAGTTCATCTAdTdT); siRNA against human Sec13 (targeting sequence GCACTCATGTTACGAGGAAdTdT); siRNA against human Sec31A (targeting sequence AACAGACAAGTTCAGCATATT dTdT) were customized as the sequences (Bioneer, Co, Korea). For improving the co-efficiency of knockdown and gene expression, plasmid DNA delivery was performed 24 hr after the siRNA transfection. Thapsigargin and Dynasore were commercially purchased (Sigma Aldrich, Co. LLC).

2. Antibodies

Antibodies were from the following sources: anti-Sec16A (KIAA0310), anti-Sec24B and anti-Sec24D (Bethyl Laboratories, INC); anti-Sec31A (BD Transduction Laboratories), anti-IRE1α, anti-myc and anti-HA (Cell Signaling Technology, Danvers, MA); anti-Flag M2, anti-γ-tubulin (Sigma); anti-Calnexin mouse monoclonal, anti-GRASP55 rabbit polyclonal (Abcam, Cambridge, MA); anti-GRASP55 monoclonal (Novus Biologicals, LLC); anti-Aldolase A, anti-ß-actin (Santa Cruz Biotechnology, SantaCruz, CA); and anti-CFTR M3A7 (Millipore, Billerica, MA). The anti-R4 polyclonal antibody was raised against peptides corresponding to amino acids at 1458-1471 of human CFTR as previously reported.[33]

3. Immunoprecipitation, Surface biotinylation and Immunoblotting

Immunoblotting and Immunoprecipitation were performed as described previously.[10] HEK293 cells transfected with appropriate plasmids were homogenized in lysis buffer containing 25 mM Tris (pH 7.4), 1% (v/v) NP40, 150 mM NaCl, 5% glycerol, and 1 mM EDTA (Roche, Applied Science, Mannheim, Germany). For co-immunoprecipitation, cell lysates (1,000 μg protein) were diluted to a final volume of 500 μL in lysis buffer and pre-cleared with control Agarose Resin (crosslinked 4% beaded agarose) for 2 h at 4 °C. To avoid co-elution of the antibody heavy and light chains that may have co-migrated with the GRASP55 bands, we immobilized 10 μg affinity-purified rabbit anti-Sec16A (KIAA0310) antibody or normal rabbit IgG (Santa Cruz Biotechnology, SantaCruz, CA) to AminoLink Plus Coupling Resin (Pierce Co-Immunoprecipitation Kit, Pierce, Rockford, IL, USA) at room temperature for 2 hr. To precipitate endogenous Sec16A, pre-cleared protein complexes were collected with antibody-coupled resin overnight at 4 °C and then washed five times with the lysis buffer; the immune complexes were eluted with 30 μL elution buffer (pH 2.8) containing primary amine and 5× lane-marker sample buffer (0.3 M Tris•HCl, 5% SDS, 50% glycerol, lane-marker tracking dye; pH 6.8) containing 100 mM DTT. Protein bands were detected by enhanced chemiluminescence, and the densities of the bands were quantified using imaging software (Multi Gauge ver. 3.0; Fujifilm, Tokyo, Japan).

The surface biotinylation assay was performed as previously described.[10] HEK293 cells

were transfected with appropriate plasmids and after 48 hr, cells were washed with phosphate buffered saline (PBS) containing 0.1mM $CaCl_2$ and $MgCl_2$ (PBS-CM plus), and then incubated with 1 mL biotin solution (0.3 mg/mL EZ-Link Sulfo-NHS-SS-Biotin in cold PBS-CM plus, Thermo Pierce) for 30 min at 4 °C. Cells were incubated with quenching buffer containing 0.5% bovine serum albumin (BSA) for 10 min and then washed three times with PBS. After cell lysis, the lysates were centrifuged at 16,000 g for 20 min at 4 °C. Resulting supernatant containing equal amount of total protein was incubated with 200 μL 10% Streptavidin agarose (Thermo Pierce). Streptavidin-bound biotinylated proteins were centrifuged and washed five times with lysis buffer and then eluted in 2x sample buffer. The following steps of the biotinylation assay were the same as for the immunoblotting procedure described above.

4. Immunocytochemistry, Confocal Microscope image acquisition and morphometric analysis

Immunocytochemistry were performed as previously reported.[10] HeLa cells were cultured on 18 mm round coverslips and fixed with -20 °C methanol for 6 min at -20 °C. The fixed cells were washed three times with PBS and then were incubated with blocking solution containing 5% horse serum, 1% BSA and 0.1% gelatin in PBS for 1 hr at room temperature. After the blocking step, cells were stained by incubating with appropriate primary antibodies and the treated with fluorophore-dye conjugated secondary antibodies. In the case of immunostaining of surface expressed protein, cells were fixed with 4% formaldehyde for 6 min at room temperature without permeablization and then stained with primary and secondary antibodies. Fluorescence images were captured using a laser scanning confocal microscope (LSM 780; Carl Zeiss, Berlin, Germany). Images were scanned using a 63x 1.4 numerical aperture (NA) oil objective lens. For distinguishing subcellular localization pattern of the cells in ER-Stress or GRASP-overepxressed condition from the control cells, zoom factor of 1 was used.

Morphometric analysis of the captured confocal images was performed by using MetaMorph Microscopy Analysis Software (version 7.1; Molecular Devices, Sunnyvale,

USA). For quantification of images under each condition, 24-bit confocal images containing red, green and blue components were primarily converted into three 8-bit mono-channel images. For the quantification of surface CFTR intensity, pixels above threshold level of 60 were defined as CFTR. The intensity profile of each single cell was presented as the standard deviation around the mean of the average intensity value for the entire region. For the analyses of the Sec16A distribution, the high-resolution images of Sec16A punctates were smoothed using a low-pass filter in MetaMorph, and pixels above the threshold level of 30 were defined as Sec16A (+). The regions of the total cell area were determined by the trace region tools of MetaMorph using the differential interference-contrast images of the cells, then the ratio of the Sec16A (+) area versus the total cell area was calculated. The distribution of Sec24 was analyzed by the same method.

The degree of colocalization between Sec16A and ER markers (or GRASP55) was quantified based on MCC (Manders' Colocalization Coefficients)[34] using the colocalization module of the ZEN 2012 software (black edition; Carl Zeiss, Berlin, Germany). For the measurement of MCC under each condition, pixels above the fluorescence threshold level of both channels (red and green) 50 were defined as the overlapping signals. Then, the average of MCC obtained from the regions of interest was calculated. For two target proteins, represented as Sec16A and ER, two different MCC values were calculated as:

$$MCC_{Sec16A\ colocalized\ with\ ER/Total\ Sec16A} = \frac{\sum_i Sec16A_{i,colocal}}{\sum_i Sec16A_i}$$

$$MCC_{ER\ colocalized\ with\ Sec16A/Total\ ER} = \frac{\sum_i ER_{i,colocal}}{\sum_i ER_i}$$

5. Internalization assay

The internalization of cell surface CFTR was performed as previously described.[35] HEK293 cells were transfected with plasmids encoding CFTR and co-transfected with or without Flag-dynamin2-K44A. After 48 hr, cells were biotinlyated with EZ-Link sulfo-NHS-SS-biotin (0.3 mg/mL in PBS-CM) for 30 min at 4 °C. Then the cells were warmed to 37 °C for the indicated times to induce internalization of surface proteins. Subsequently, the biotin of sulfo-NHS-SS-biotinlyated proteins were stripped by washing with the sodium 2-

mercaptoethanesulfonate (MESNA) stripping buffer (50 mM MESNA, 150 mM NaCl, 1 mM EDTA, 0.2% BSA and 20 mM Tris of pH 8.6) for 15 min for four times. After washing for three times with PBS, the cells were lysed with lysis buffer and then were centrifuged at 16,000 g for 20 min at 4 °C. Resulting supernatant containing equal amount of total protein was incubated with 200 μL 10% Streptavidin agarose (Thermo Pierce) overnight at 4 °C with gentle agitation. Streptavidin-bound biotinylated proteins were centrifuged and washed five times with lysis buffer and then eluted in 2x sample buffer. The following steps of the biotinylation assay were the same as for the immunoblotting procedure described above.

6. Immunogold labeling and Transmission electron microscopy (TEM)

HeLa cells were fixed and performed with cyroimmuno-EM labeling as described in Martinez-Menárguez et al.[36] HeLa cells were grown in 100mm dish were transfected with HA-Arf1Q71L plasmid or empty plasmid and after expressed for 18 hr, cells were fixed with 4% paraformaldehyde and 0.1% glutaraldehyde in PBS buffer (pH 7.4) at 4℃ for 20min. The fixed cells were embedded in 10% gelatin and small blocks were infused overnight with 2.3M sucrose. Finally, frozen were performed in liquid nitrogen. For electron microscopy studies, 50 nm ultrathin cyrosections were cut at -120 °C using a Leica UCT7 cyro-ultramicrotome (Leica, Vienna, Austria). Ultrathin sections were transferred from the diamond knife onto Formvar-coated copper slot grids using 2.3 M sucrose: 2% methylcellulose (1:1). Rabbit polyclonal GRASP55 antibody (Abcam, diluted 1:50) was used as primary antibody and to detect primary antibody, Protein A-10nm gold conjugate (from Dept. of Cell Biology, Utrecht School of Medicine, Utrecht, Netherlands) was used. Both GRASP55 antibody and Protein A gold were diluted in 0.1% BSA-c (Aurion, Netherlands) in PBS. For immunogold labeling experiments, the ultrathin cryosections were firstly blocked with 0.1% cold fish gelatin and 5% BSA for 10min and then were incubated with GRASP55 antibody for 30min, continually were incubated with protein A-gold for 30 min. The grids were stained in 4% neutral uranyl acetate and embedded in 2% methylcellulose containing 0.3% uranyl acetate as previously described.[37] Immuno-electron microscopy was conducted as examining the grids at 120 kV using a Tecnai G^2 Spirit Twin Transmission Electron Microscopy (FEI Company, USA).

7. Quantitative real-time PCR (qPCR)

Purified RNA samples from HEK293 cells which endogenous Sec23A, Sec24A, Sec13A were silenced with specific siRNA were reverse-transcribed using RNA to cDNA EcoDry™ Premix (Clontech Laboratories, Takara Bio company). The total reaction volume was adjusted to 20 μL with RNase-free water after mixing 100 ng cDNA, 1 μL forward primer and 1 μL reverse primer for each, 10 μL 2x SYBR premix Ex Taq and 0.4 μL 50x ROX reference dye (Takara Bio Inc). Amplification was performed under the following cycling conditions: 95 °C for 15 min followed by 40 cycles of 95 °C for 15 sec and 60 °C for 40 sec. Triplicate analyses were performed for each cDNA. Relative mRNA expression levels were calculated via the comparative threshold cycle (C_t) method with GAPDH as control as follows: $\Delta C_t = C_t$ (GAPDH)-C_t (target gene). The fold-change in gene expression normalized to GAPDH and relative to the control sample was calculated as $2^{-\Delta\Delta Ct}$.

8. Biological and technical replication

Biological replicates are parallel measurements of biologically distinct samples that capture random biological variation. The samples for each biological replicate were prepared from cells grown at different times. Technical replicates are repeated measurements of the same sample of each biological replicate.

In the case of western blot data, almost the whole amount of proteins from one biological replicate was used for surface biontinylation assay or immunoprecipitaton assay. Therefore, only one technical replicate was performed for each biological replicate. The sample size described above refers to the number of biological replicates. In the case of qRT-PCR experiments, three equal-sized aliquots of cDNA from the same biological replicate are used as the template in individual PCR reactions. For each biologically distinct condition, average value of technical replicates was computed as a single data point of one biological replicate. The sample size described above refers to the number of biological replicates. In the case of immunofluorescence experiments, at least five biological replicates were used. For each biological distinct condition, images from 5-10 cells were averaged and used for

the single data point of statistical analyses.

9. Criteria for exclusion/inclusion of data

The outlier data are not ‘errors’ but just the observations are distant from the mean of observations. In the present study, once the correct experimental conditions were confirmed (e.g. expression of HA-Arf1-Q71L or knockdown of Sec16A in western blotting of cell lysates), not any outlier data was excluded.

10. Statistical analysis

All experiments were performed at least three times independently for each condition and present as the mean ± SEM (standard error of the mean). Statistical analysis was performed using Student’s t-tests or with analysis of variance followed by Dunnet’s multiple comparison tests as appropriate; $p < 0.05$ was considered statistically significant. Calculations were performed using GraphPad Prism5 software (GraphPad Software,Inc., La Jolla,CA).

III. RESULTS

1. Sec16A affects both conventional secretion of CFTR and unconventional secretion of ΔF508-CFTR

Wild type CFTR undergoes Golgi-mediated complex glycosylation (Figure 1A, band C) and ER-mediated core-glycosylation (Figure 1A, band B). It has been shown that ER export of Golgi protein GalNAc-T2-GFP was abolished by Sec16A depletion.[38] Brefeldin A (BFA) treatment led to redistribution of GalNAc-T2-GFP to ER and returned to Golgi after BFA removal[39] in control cells treated with nonspecific siRNA, in contrast, knockdown of Sec16A led to accumulation of GalNAc-T2-GFP in the juxtanuclear Golgi region[38], as reported earlier. In an effort to identify the role of Sec16A in conventional secretion of CFTR, RNAi-mediated knockdown of Sec16A was performed in HEK293 cells. Silencing of Sec16A by small interfering RNA (siRNA) strongly reduced the surface expression of complex-glycosylated CFTR (band C) (Figure 1A, B), indicating that ER-to-Golgi mediated transport of CFTR was abolished by depletion of Sec16A. Moreover, surface expression of core-glycosylated immature form of CFTR which was transported through Golgi-bypass unconventional secretion pathway was also inhibited by silencing of Sec16A (Figure 1A, lane 3-4). Arf1-Q71L is a dominant negative mutant of COPI component restricted to GTP-bound form. Expression of Arf1-Q71L could induce ER-to-Golgi blockade[40,41] resulting in unconventional secretion of core-glycosylated CFTR to the cell surface.[10] In contrast, the surface expression of ΔF508-CFTR (Figure 1C, lane 3) under the condition of Arf1-Q71L induced ER-to-Golgi blockade was abolished by depletion of Sec16A by siRNA (Figure 1C, lane 4). In order to rule out the possibility that these rescue events were resulted from internalization, we examined the surface expression of core-glycosylated CFTR with treatment of dynamin inhibitors including dynasore and the dominant-negative mutant of dynamin (dynamin2-K44A) to inhibit the protein endocytosis process.[42,43] Results of the internalization assays showed that treatment of dynasore (80 μM, 12 hr) (Figure 4B) and expression of dynamin2-K44A (Figure 4C) reduced the internalization of wild-type CFTR. Even though these treatment induced an increment in cell-surface expression of transferrin receptor and complex-glycosylated wild-type CFTR (Figure 5A, B), dynasore treatment and

dynamin2-K44A expression neither resulted in cell-surface expression of core-glycosylated CFTR nor interfered the Arf1-Q71L-mediated unconventional secretion of ΔF508-CFTR (Figure 5C, D).

As an additional and verification approach, we also investigated the function of core COPII components in the secretion of ΔF508-CFTR by RNAi screening. Sec23-24 and Sec13-31 complexes are downstream COPII coat proteins defining the later structure of ER exit sites (ERES) on the basis of that the platform protein Sec16A defines the tER.[29] As shown in Figure 2, depletion of Sec16B and the isoforms of COPII components including Sec23, Sec24, Sec13 and Sec31 siRNA do not alter the Arf1-Q71L-mediated cell-surface expression of ΔF508-CFTR. The knockdown efficiency of siRNAs was confirmed through quantification of the mRNA or protein expression of each target gene by quantitative real-time PCR and immunoblotting (Figure 3). These results altogether demonstrate that Sec16A is the unique element which was responsible for both conventional and unconventional secretion of CFTR.

Next, we confirmed the role of Sec16A in surface expression of CFTR and ΔF508-CFTR by using the immunocytochemistry approach. For morphological analysis, in order to prevent the cells from deranging or losing during the immunocytochemistry, HeLa cells were utilized instead of HEK293 cells taking advantage of the feature of HeLa cells could attach more firmly to coverslips. HeLa cells were firstly transfected with scrambled or Sec16A-specific siRNA, after 24 hr, HA tagging at the extracellular loop of wild type-CFTR or ΔF508-CFTR were transiently transfected and then were expressed for another 24 hr. Subsequently, non-permeabilized fixation was performed with 4% paraformaldehyde for 6 min at room temperature to circumvent the possibility of destruction of membrane integrity. HA-epitopes exposed at the cell surface would be labeled and the surface expressed CFTR or ΔF508-CFTR could be detected. In control cells expressing wild type-CFTR, surface expressed CFTR were detected in non-permeabilized cell membrane (Figure 6A, green fluorescence image). In accordance with the surface biotinylation result (Figure 1A, lane1), ΔF508-CFTR could not reach the plasma membrane in normal condition based on non-fluorescence signal in the cell surface (Figure 6B) despite ΔF508-CFTR expression could be

detected by anti-R4 antibody staining after membrane was permeablized (Figure 6B, red fluorescence image) after the surface staining with anti-HA antibody was completed. On the contrary, when the ER-to-Golgi conventional secretion was blocked by expression of dominant negative mutant Sar1-T39N which is the GDP-restricted Sar1 GTPase,[44] surface expressed ΔF508-CFTR could be observed in non-permeabilized cells (Figure 6C, green fluorescence image). However, the ER-to-Golgi blockade mediated rescue of ΔF508-CFTR was notably reduced by silencing of Sec16A by siRNA (Figure 6D, E). In a word, these results indicate that Sec16A is required for the unconventional secretion of CFTR but the other COPII components are not needed.

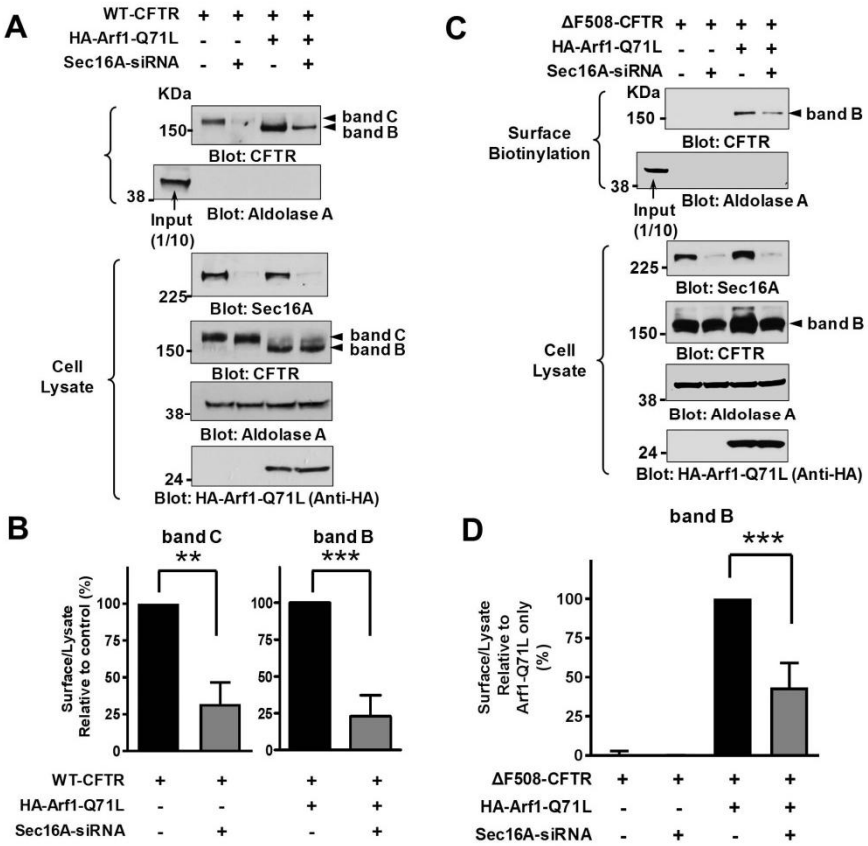

Figure 1. Sec16A-depletion inhibited the surface expression of both complex-glycosylated CFTR and core-glycosylated CFTR. Surface biotinyation of CFTR or ΔF508-CFTR. **(A, C)** Proteins extract from HEK293 cells were firstly transfected with equal amount of control scrambled siRNA or Sec16A-specific siRNA (150 nM), after 24 hr, transfected with wild type **(A)** or ΔF508-CFTR **(C)**. Arf1-Q71L overexpression was used to block the ER-to-Golgi conventional trafficking. Surface-biotinlyated proteins and the whole proteins were immunoblotted with anti-Sec16A, anti-M3A7 and anti-HA antibodies. In each experiment, cell surface specific labeling of proteins was confirmed by the absence of cytosolic protein AldolaseA in biotinlyated fraction. RNAi-mediated knockdown of Sec16A abolished conventional surface secretion of WT-CFTR **(A)**. Surface expression of immature core-glycosylated b form of WT-CFTR **(A)** or ΔF508-CFTR **(C)** were also reduced by silencing of Sec16A under the condition of Arf1-Q71L overexpression induced blockade of conventional ER-to-Golgi traffic. Multiple experiments (n=4) are summarized in **(B, D).** Surface-proteins versus cell lysates were quantified and data were shown as mean ±SEM. $^{**}p < 0.01$, $^{***}p < 0.001$, ns: no significant differences. band B: immature ER core-glycosylated CFTR; band C: mature complex-glycosylated CFTR. See Table 1-2 for sample size, replication and statistical information.

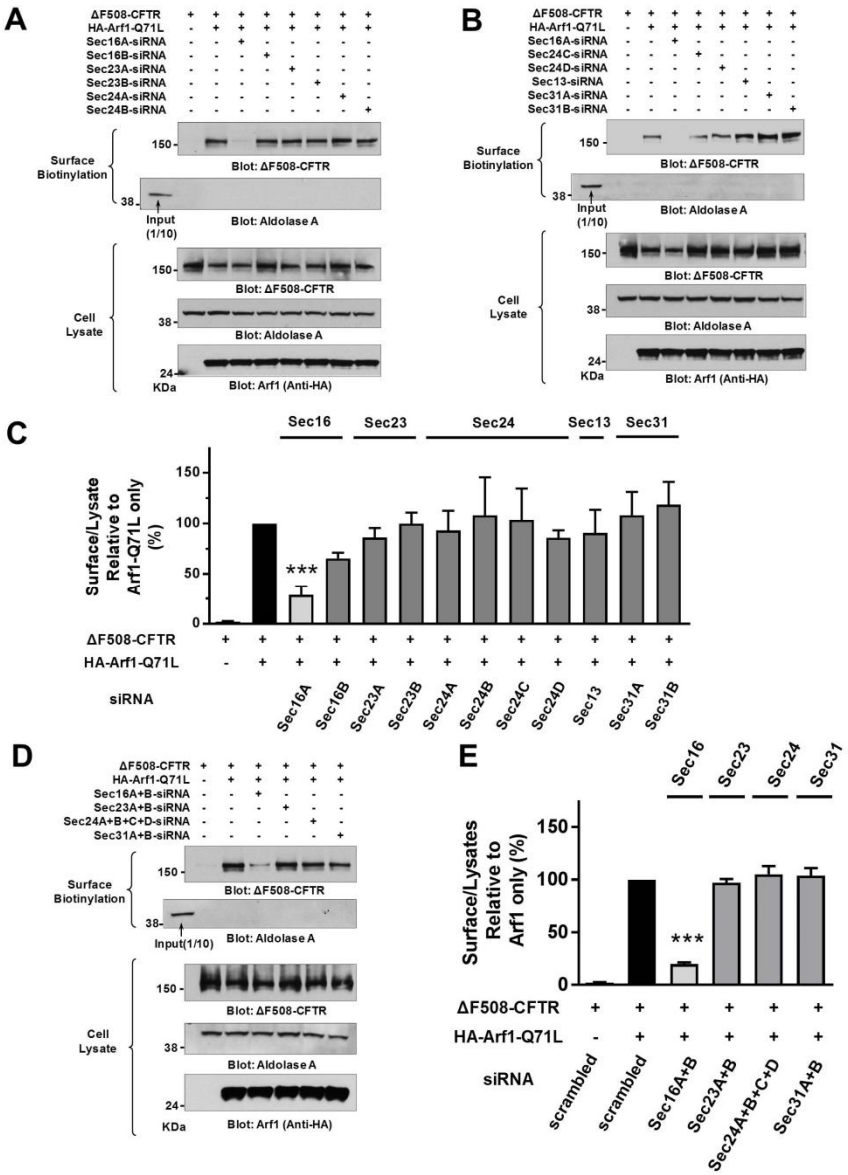

Figure 2. COPII core components are not required for Arf1-Q71L-induced cell-surface expression of ΔF508-CFTR. (**A, B**) Representative surface biotinylation assays of single gene knockdown. The ER-to-Golgi blockade induced unconventional secretion of ΔF508-CFTR was not affected by knockdown of COPII component proteins. Surface biotinylation was performed after transfection with control scrambled siRNA or siRNAs specific for Sec16, Sec23, Sec24, Sec13 and Sec31 (150 nM for each). Results of multiple experiments are summarized in (**C**). (**D**) Representative surface biotinylation assays of the combinatorial gene knockdown on the same gene family. Results of multiple experiments are summarized in (**E**). Data are shown as mean ±SEM. ***$p < 0.001$. See Table 1-2 for sample size, replication and statistical information.

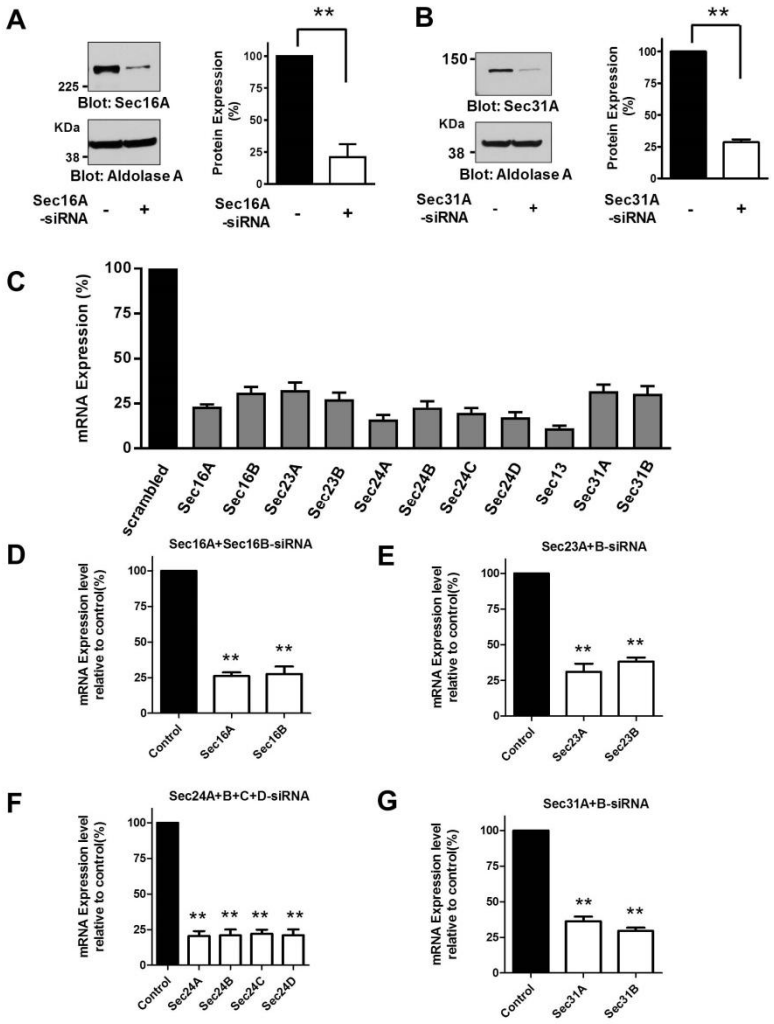

Figure 3. Validation of siRNAs targeting Sec16A and core COPII components (**A, B**) HEK293 cells were transfected with each siRNA for 48 hr and then protein samples were prepared. A 70–90% depletion of Sec16A (**A**, mean ± SEM, n = 3) and Sec31A (**B**, mean ± SEM, n = 3) was confirmed by immunoblotting, (**C)** Validation of each siRNA was performed by quantitative real-time PCR based mRNA quantitation. Single gene siRNAs specifically targeting human isoforms of Sec16 and all core COPII components including Sec23, Sec24, Sec13, and Sec31 were transfected to HEK293 cells for 48 hr and then RNA samples were extracted from the cells under each condition. (**D-G**) Validation of siRNAs under conditions of multiply knockdown of Sec16 and COPII components on the same gene family was performed by quantitative real-time PCR based mRNA quantitation . (mean ± SEM, n = 3). $^{**}p < 0.01$. See Table 1-2 for sample size, replication and statistical information.

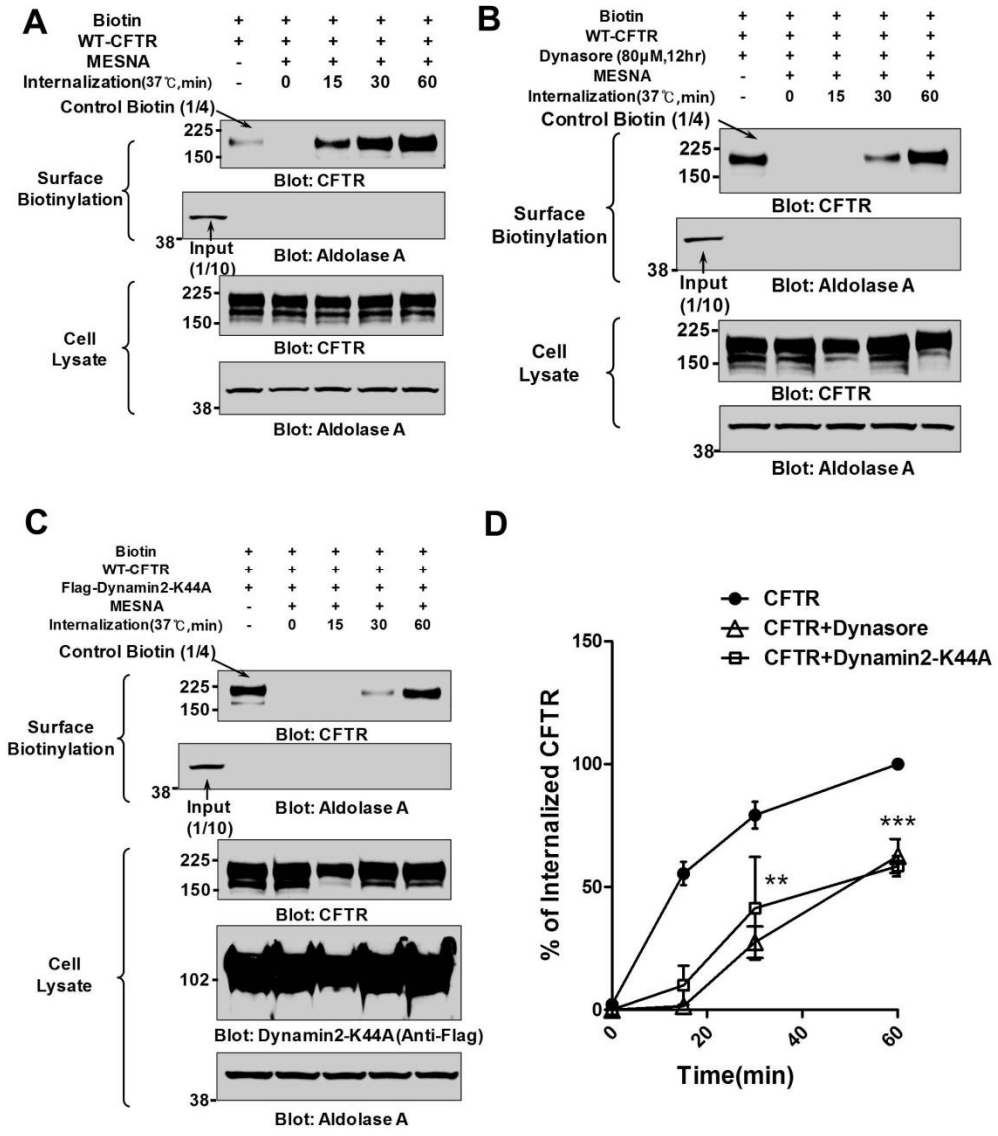

Figure 4. Internalization of CFTR was inhibited by dynamin inhibitors. (A-C) The internalization assay of cell surface CFTR was performed in HEK293 cells with or without **(A)** dynamin inhibitors including dynasore (80 μM, 12 hr) treatment **(B)** or expression of dynamin2-K44A **(C)**. Dynasore and dynamin2-K44A are inhibitors of the dynamin-mediated internalization. Cell surface proteins were biotinylated and then internalized for indicated times at 37 °C. Proteins remaining at the cell surface were stripped of biotin with MESNA stripping buffer. **(D)** Quantification of results of multiple experiments (mean ± SEM, n = 3) are summarized. $^{**}p < 0.01$, $^{***}p < 0.001$. See Table 1-2 for sample size, replication and statistical information.

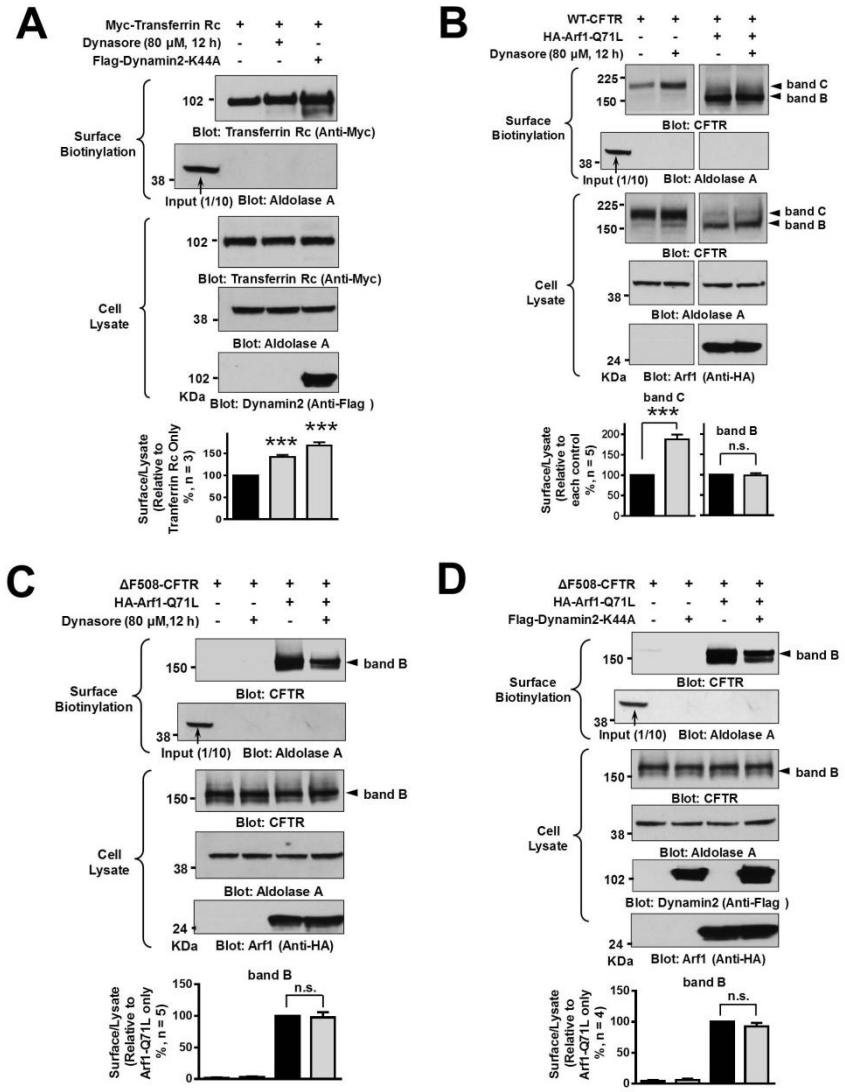

Figure 5. Arf1-Q71L-induced surface expression of core-glycosylated CFTR is not influenced by inhibition of internalization. HEK293 cells were transfected with plasmids expressing transferrin receptor or CFTR, and a surface biotinylation assay was performed 24 hr after transfection. **(A)** Cell-surface expression of transferrin receptor (Rc) was increased by dyasore and dynamin2-K44A. **(B)** Surface expression of band C form of wild-type CFTR was increased by dynasore treatment; however, the Arf1-Q71L-mediated surface expression of band B form of wild-type CFTR was not affected. **(C)** Dynasore and **(D)** dynamin2-K44A neither induced the surface expression of ΔF508-CFTR, nor influenced the Arf1-Q71L –induced surface expression of ΔF508-CFTR. Quantification of results of multiple experiments are summarized under each blot. ***$p <$ 0.001, n.s.: not significant. See Table 1-2 for sample size, replication and statistical information.

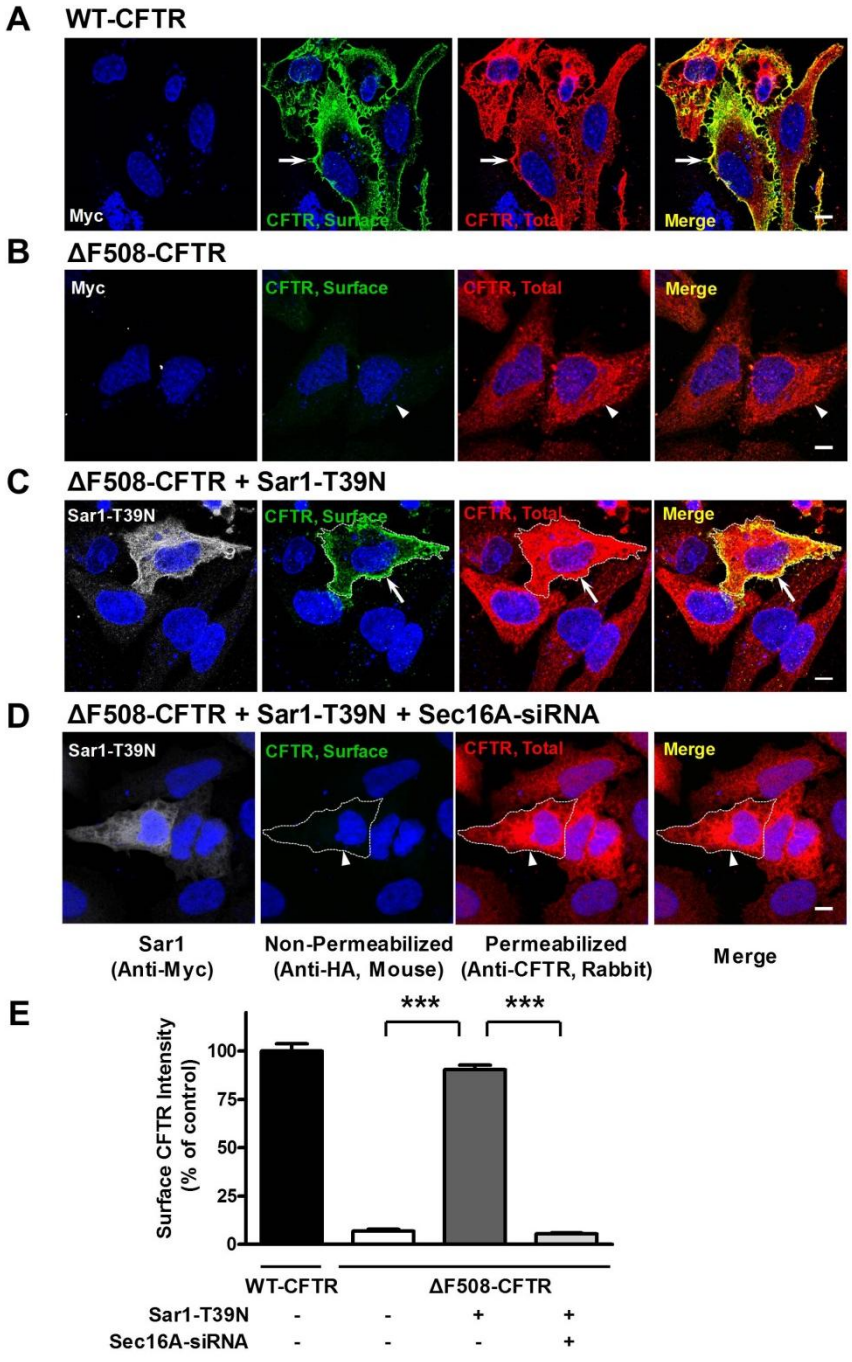

Figure 6. Silencing of Sec16A inhibits unconventional trafficking of ΔF508-CFTR to the cell surface. (A-D) Representative immunofluorescence images of wild-type (WT) or ΔF508-CFTR. Non-permeabilized immunostaining of surface expressed CFTR was performed. After Sec16A

siRNA was transfected and expressed for 24 hr, DNA plasmids of HA-tagged at the extracellular loop of CFTR or ΔF508-CFTR were transfected to HeLa cells. The cells were stained with HA antibody after 4% paraformaldehyde fixation without permeabilization procedure. Following the surface staining of CFTR (green), treatment of the same cells with methanol was performed to permeablize both plasma membrane and intracellular membranes. The cells were stained with anti-R4 antibody to confirm the expression of CFTR or ΔF508-CFTR (red). Sar1-T39N were stained with anti-myc antibody and showed as grey pseudo color image. WT-CFTR well expressed on the surface **(A)**, in contrast, ΔF508-CFTR was retained in the ER **(B)**. When ER-to-Golgi was blocked by Sar1-T39N, ΔF508-CFTR was rescued to the cell surface **(C)**. However, silencing of Sec16A by siRNA abolished the surface expression of ΔF508-CFTR **(D)**. **(E)** Quantification of surface CFTR intensity. Data are shown as mean ± SEM from three independent experiments (each comprising analysis of 20-30 cells). Arrows indicate surface expressed CFTR or ΔF508-CFTR. Arrowheads indicate the cells do not express surface CFTR. Scale bar, 10 μm. ***$p < 0.001$. See Table 1-2 for sample size, replication and statistical information.

2. Requirement of Sec16A in GRASP-mediated unconventional secretion of ΔF508-CFTR

Given recent evidences showed that overexpression of GRASPs could also activate the unconventional secretion of ΔF508-CFTR.[10] Furthermore, we investigated whether Sec16A is also involved in GRASP-mediated unconventional secretion pathway. Three different kinds of plasmids encoding GRASP55 including Myc-tagging at the N-terminus of GRASP55, Myc-tagging at the C-terminus of GRASP55 and GRASP55 without any tag were co-transfected with ΔF508-CFTR to HEK293 cells after Sec16A siRNA was transfected and expressed for 24 hr. Depletion of Sec16A by small interfering RNA significantly reduce the surface expression of ΔF508-CFTR which was induced by overexpression of GRASP55 (Figure 7), suggesting that Sec16A plays a significant role in establishment of the platform for initiating GRASP-mediated unconventional secretion of ΔF508-CFTR.

To elucidate the platform role of Sec16A in GRASP-mediated unconventional secretion

pathway, immunoprecipiatation assay was performed to assess the protein-protein interaction between GRASP55 and Sec16A. When co-expressed in HEK293 cells, GRASP55 weakly interacted with Sec16A in normal condition (Figure 8A, line 2). However, interaction between Sec16A and GRASP55 was enhanced significantly when ER-to-Golgi blockade was induced by Arf1-Q71L expression (Figure 8A, B). Taken together, we can make a conclusion that assembly of large complexes containing GRASP55 and Sec16A would be enhanced by ER-to-Golgi blockade to initiate the formation of unconventional secretion vesicles transporting ΔF508-CFTR.

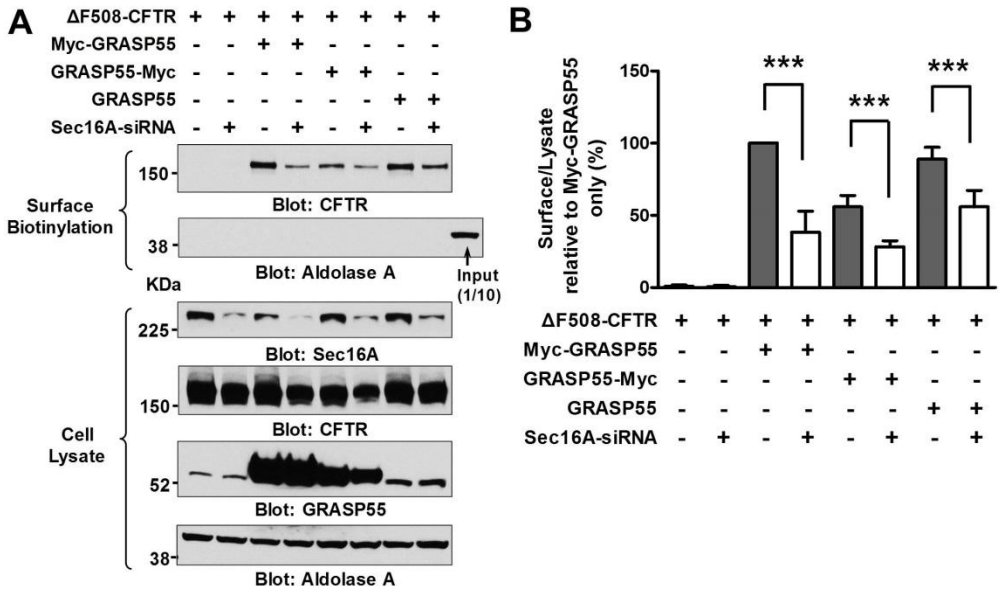

Figure 7. Depletion of Sec16A inhibited GRASP-mediated unconventional secretion of ΔF508-CFTR. (A) Surface biotinylation of ΔF508-CFTR. HEK293 cells were transfected equally with scrambled siRNA or Sec16A siRNA 24 hr before transfection of plasmids encoding ΔF508-CFTR and GRASPs. After 48 hr, surface biotinylation was performed. Overexpression of three different variants of GRASP55 (including Myc tagging at N-terminus of GRASP55, Myc tagging at C-terminus of GRASP55 and GRASP55 without any tag) induced cell surface expression of ΔF508-CFTR. Sec16A depletion diminished GRASP55-mediated surface rescue of ΔF508-CFTR. **(B)** Surface-proteins versus cell lysates were quantified and multiple experiments are summarized. Data are shown as mean ± SEM (n=3). ***$p < 0.001$. See Table 1-2 for sample size, replication and statistical information.

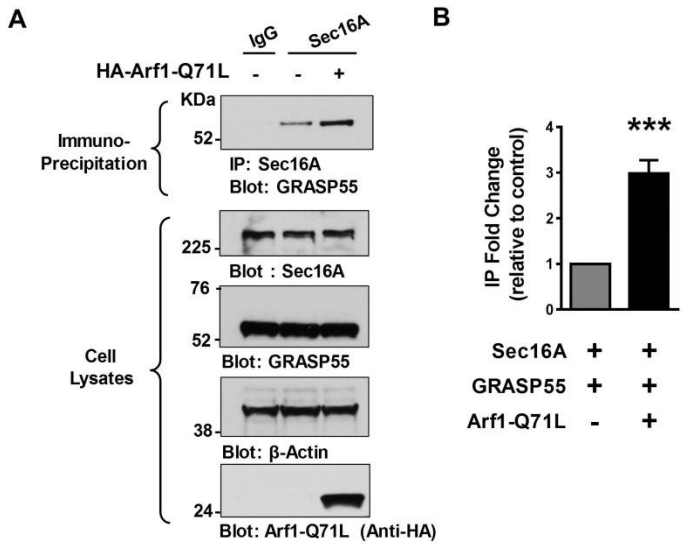

Figure 8. Protein-protein interaction between Sec16A and GRASP55 was increased by ER-to-Golgi blockade. (**A-B**) The Co-immunoprecipitation experiments with Sec16A and GRASP55 were performed in HEK293 cells. Protein samples were precipitated with anti-Sec16A (KIAA0310) and blotted with anti-GRASP55. A representative coimmunoprecipitation result is shown in (**A**), and fold change relative to control was quantified and results of multiple experiments (n = 3) are summarized in (**B**). ER-to-Golgi blockade induced by Arf1-Q71L increased the association between Sec16A and GRASP55. ***$p < 0.001$: difference from each control. See Table 1-2 for sample size, replication and statistical information.

3. Sec16A re-localizes and co-localizes with GRASP55 during the unconventional secretion of ΔF508-CFTR

To investigate the relationship between GRASP55 and Sec16A, we examined the subcellular localization of GRASP55 and Sec16 in HeLa cells. Previous research showed that in Drosophila S2 cells, dGRASP localizes both to Golgi membranes and the ER exit sites.[45] When it comes to mammalian model, in control HeLa cells, Sec16A displayed typical ERES localization that mainly concentrated adjacent to the nucleus but only a minority of puncta dispersed in the peripheral area, and GRASP55 showed typical perinuclear ribbon-like structure of the Golgi apparatus (Figure 9A). Nevertheless, GRASP55 redistributed overall the whole cell increasing the colocalization with puncta of

Sec16A especially in the peripheral region when ER stress was induced by treatment of thapsigargin which depletes calcium storage in the ER lumen (Figure 9B) and co-expression with Arf1-Q71L or Sar1-T39N which induces ER-to-Golgi blockade. (Figure 9C, D). Furthermore, transmission electron microscopy (TEM) observation supported that Arf1-Q71L induced ER-to-Golgi blockade results in redistributing of Golgi protein GRASP55 from the Golgi to the ER, in which the ERES protein Sec16A localizes (Figure 10).The relocalization of Sec16A accompanying with GRASP55 in response to ER stress raises a question whether Sec16A opens the gate for GRASP55 to mediate the unconventional secretion of ΔF508-CFTR.

Next, to identify the role of Sec16A in the unconventional ΔF508-CFTR secretion, we compared the cellular localization of Sec16A, GRASP55 and ΔF508-CFTR under various conditions stimulating unconventional secretion of ΔF508-CFTR. Arf1-Q71L induced blockade of ER-to-Golgi resulted in the surface expression of ΔF508-CFTR in HeLa cells (Figure 11A, B). Moreover, the localization of Sec16A got changed by Arf1-Q71L. Sec16A puncta mainly concentrated in the juxtanuclear region (Figure 11A and HA-negative cells in Figure 11C, arrowheads) in normal condition, in contrast, Sec16A puncta dispersed into more peripheral regions (Figure 11B and HA-positive cells in Figure 11C, arrows) when the ER-to-Golgi transport was blocked by Arf1-Q71L and the Sec16A puncta appeared in > 80% of the cytoplasmic area (Figure 11D). These results are comparable with a recent finding which reported that ER relocalization of GRASP is a requisite for unconventional secretion of ΔF508-CFTR.[46] What's more interesting, in HeLa cells with a high level of GRASP55-Myc expression, which induces unconventional secretion of ΔF508-CFTR (Figure 13B), the puncta of Sec16A and GRASP55 were noticeably redistributed to the whole cell area (Figure 12C, arrows). In contrast, in the cells with a low level of GRASP55-Myc expression, which does not induce unconventional secretion of ΔF508-CFTR (Figure 13A), GRASP55 expressed at the typical perinuclear Golgi apparatus (Figure 12B) and the puncta of Sec16A mainly concentrated in the typical perinuclear ERES region to facilitate conventional ER-to-Golgi transport (Figure 12A, B). Additionally, immunofluorescence colocalization analyses which assesse the pixel colocalization correlation between Sec16A and ER markers (ER-

YFP and calnexin) revealed that the relocalized Sec16A puncta were highly colocalized with the ER-marker proteins, suggesting that Sec16A relocalized to the peripheral ER area (Figure 14). The peripheral localization of Sec16A increased Manders' Colocalization Coefficient (MCC) due to an increment in the co-incident coefficient between the fractions of Sec16A and ER marker proteins (Figure 14C, G). Altogether, ER-to-Golgi blockade and GRASP55 overexpression stimulate the localization change of Sec16A and GRASP55 and facilitate the assembly of large complexes containing Sec16A, GRASP55 and ΔF508-CFTR.

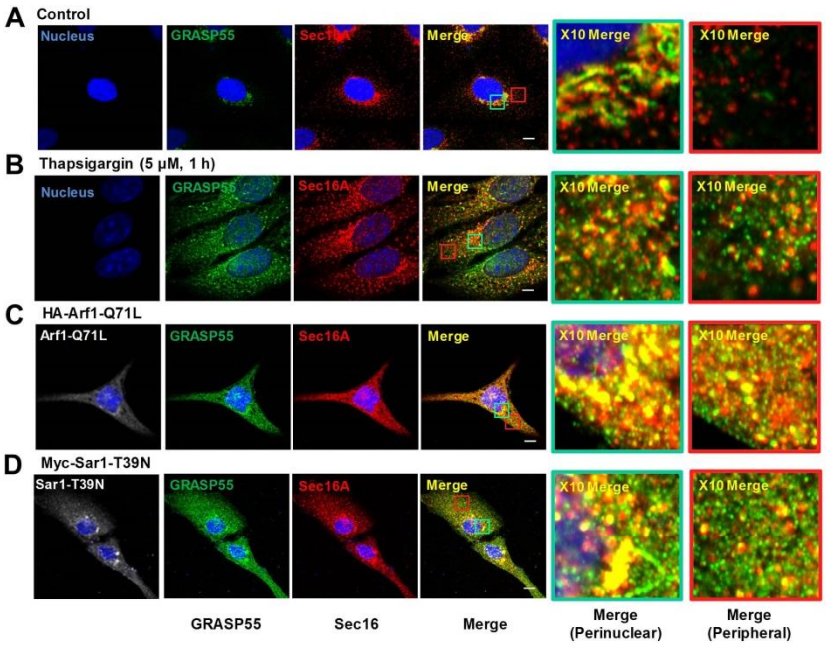

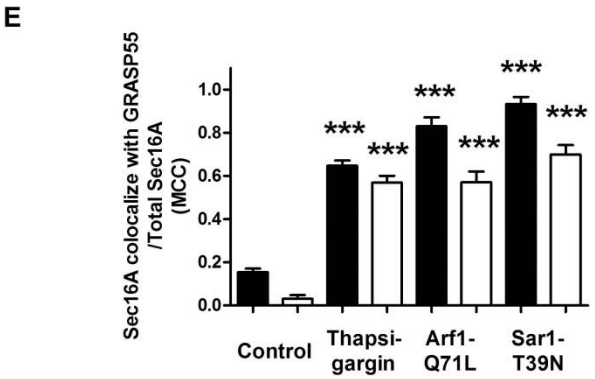

Figure 9. Colocalization of Sec16A and GRASP55. (**A–D**) The cellular localization of Sec16A and GRASP55 was analyzed using immunocytochemistry in HeLa cells. Representative immunofluorescence images are shown. Endogenous GRASP55 was labeled with fluorophore-tagged antibodies (green), and Sec16A was labeled with fluorophore-tagged antibodies (red). Some cells were cotransfected with Arf1-Q71L (**C**) or Sar1-T39N (**D**) to induce ER-to-Golgi blockade. The induction of ER stress (thapsigargin) (**B**) or ER-to-Golgi blockade (Arf1-Q71L or Sar1-T39N) significantly increased the colocalization of Sec16A and GRASP55 in both the perinuclear (green box) and the peripheral (red box) regions. (**E**) Quantification of multiple experiments (mean ± SEM, n = 5, each comprising analyses of 5–10 cells) analyzing the Manders' colocalization coefficient (MCC) of fraction of Sec16A in compartments containing GRASP55 are summarized. The precise analysis procedures were described in the Materials and Methods. Scale bar: 10 μm, ***$p < 0.001$: difference from each control. See Table 1-2 for

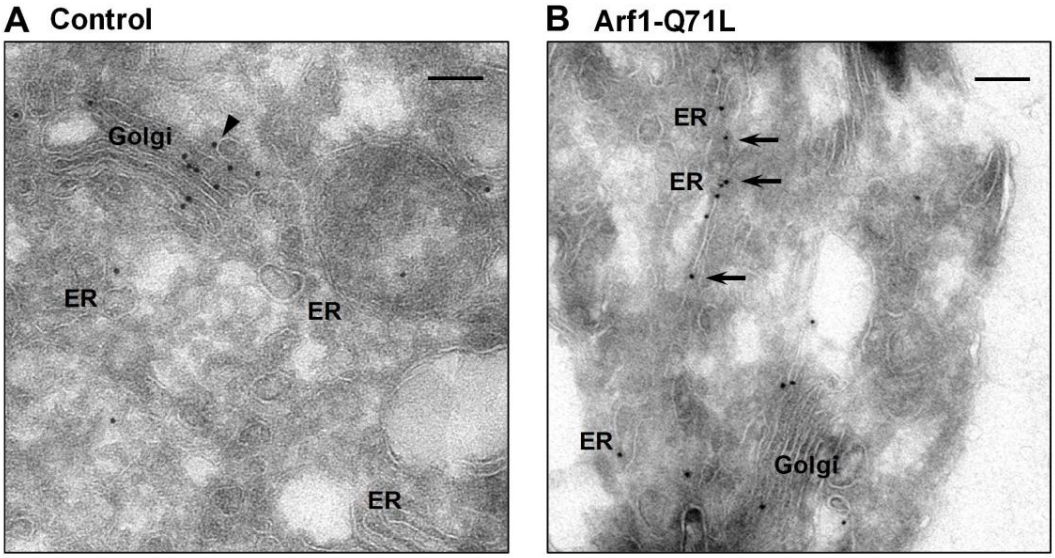

Figure 10. Electron Microscope observation of the immunogold labeled GRASP55. Transmission electron microscopy (TEM) observation showed the localization of GRASP55 in normal condition **(A)** and in Arf1-Q71L induced ER-stress condition **(B).** GRASP55 (10 nm gold particles) was immunolabeled on the ultrathin cryosections of HeLa cells. GRASP55 immunogold particles were found on the Golgi membrane (arrowhead) in the control cells **(A).** Arf1-Q71L induced ER-to-Golgi blockade induced GRASP55 gold particles redistributed to ER (arrows) **(B).** The precise experiment procedures were described in the Materials and Methods. Scale bar: 200 nm.

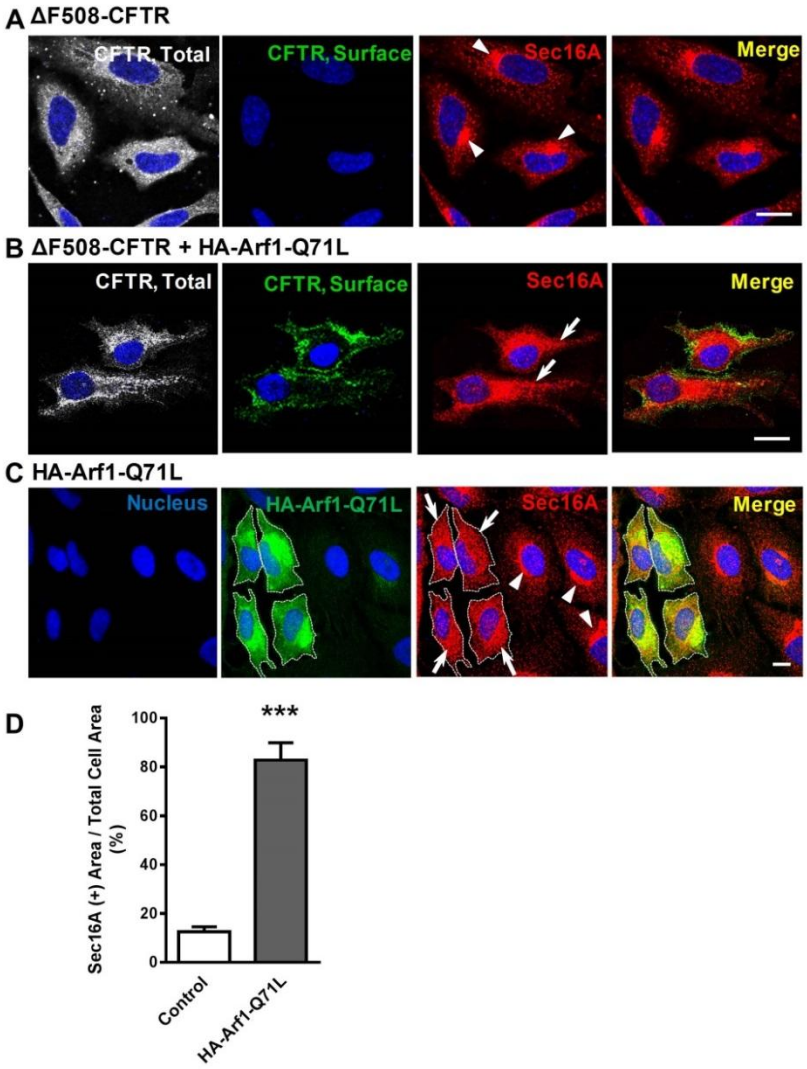

Figure 11. Arf1-Q71L-induced unconventional secretion of ΔF508-CFTR was accompanied by localization change of Sec16A. (A, B) Representative immunofluorescence images of Sec16A and ΔF508-CFTR in normal condition and under the condition of Arf1-Q71L induced ER-to-Golgi blockade. HeLa cells were transfected with plasmids of HA-tagged at the extracellular loop of ΔF508-CFTR with empty vector or Arf1-Q71L. Before cell membrane was permeabilized, ΔF508-CFTR expressed at the cell surface was stained with anti-HA antibody (green). After cell membrane was permeabilized, total ΔF508-CFTR was stained with anti-M3A7 antibody (grey) and Sec16A was stained with anti-Sec16A (KIAA0310 antibody) (red). Sec16A puncta were localized mainly at the juxtanuclear region (arrowhead) in control cells **(A)** where ΔF508-

CFTR could not reach the cell surface**.** Sec16A puncta were relocalized to the whole cell area (arrow, red) **(B, C)** when ER-to-Golgi blockade was induced by Arf1-Q71L expression and the unconventional secretion of ΔF508-CFTR was evoked (green) **(B)**. **(C, D)** Localization change of Sec16A in cells expressing Arf1-Q71L (white dotted line) was distinguished from that in cells without of expressing Arf1-Q71L. (C) Representative immunofluorescence images are shown in **(C)** and the morphometric analysis of multiple experiments were summarized in **(D)**. Data are shown as mean ± SEM (n=5, each comprising analyses of 5-10 cells). Scale bar: 10 μm. ***$p < 0.001$. See Table 1-2 for sample size, replication and statistical information.

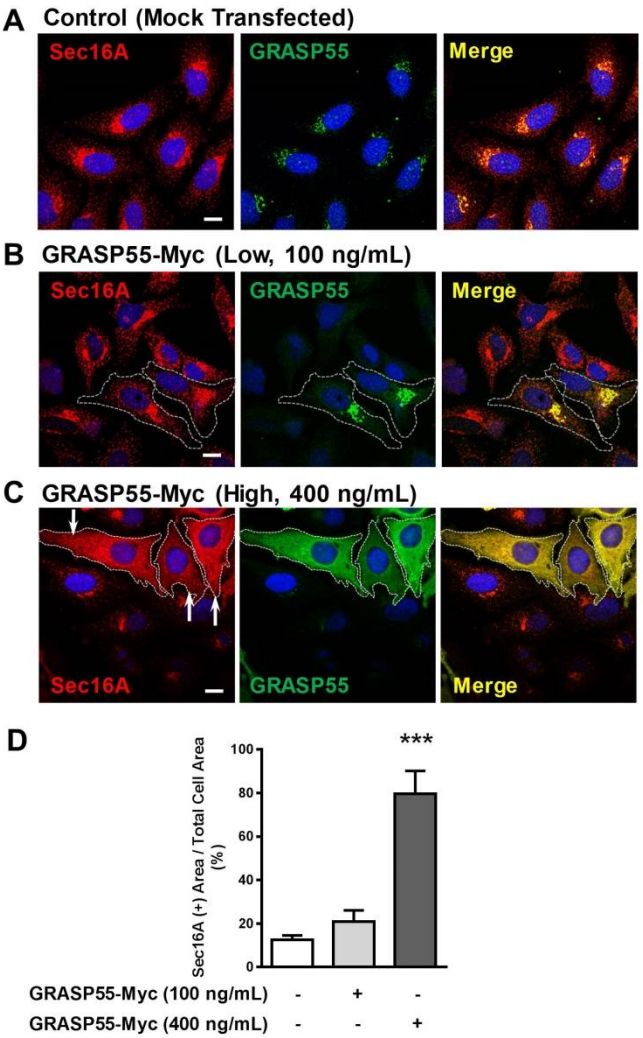

Figure 12. GRASP55-mediated unconventional secretion of ΔF508-CFTR was accompanied by relocalization of Sec16A. (A-C) Representative immunofluorescence images showed localization

of Sec16A in normal condition and in conditions of expression of exogenous GRASP55-Myc. HeLa cells were transfected with empty plasmids (**A**), GRASP55-Myc (low 100 ng/mL) (**B**) or GRASP55-Myc (high 400 ng/mL) (**C**).The cells were fixed after 24 hours and then were immunostained with anti-Sec16A and anti-GRASP55 or anti-myc (GRASP55). Cells express exogenous GRASP55 or Arf1-Q71L were labeled with white dotted lines to compare with the control cells in each view of images. Arrows indicate the puncta of Sec16A dispersed to the periphery of the cells expressed with high amounts GRASP55-Myc. **(D)** Sec16A dispersion level was quantified as percentage of Sec16A (+) area versus total cell area. Results of multiple experiments (mean ± SEM, n=5~10) were summarized. Scale bars: 10 μm. ***$p < 0.001$. See Table 1-2 for sample size, replication and statistical information.

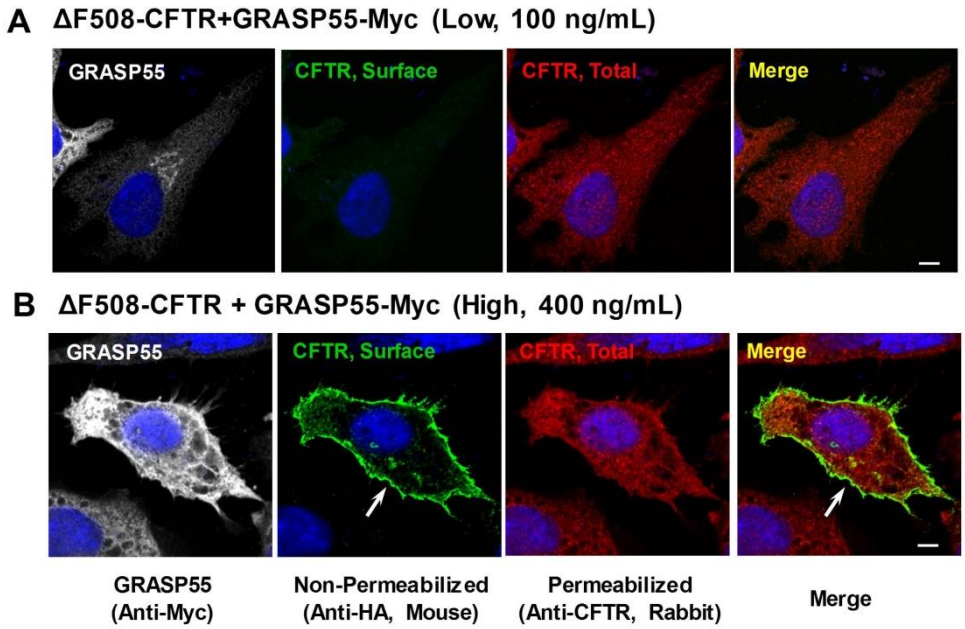

Figure 13. High level of GRASP55 expression mediated the cell-surface rescue of ΔF508-CFTR. (A, B) Cell-surface expressed HA-tagged at the extracellular loop of the ΔF508-CFTR (green) was immunolabeled with anti-HA antibodies without permeablization procedure after fixation of the HeLa cells with 4% paraformaldehyde. Then, after permeablization, the total CFTR (red) was immunostained with anti-R4 antibodies. **(B)** High-level expression of GRASP55-Myc (400 ng/mL) (grey) could rescue ΔF508-CFTR to the cell surface but **(A)** low-level expression of GRASP55-Myc (100 ng/mL) (grey) was not sufficient to rescue ΔF508-CFTR. Arrows indicate surface expression of ΔF508-CFTR. Three independent experiments showed reproducible results. Scale bars: 5 μm.

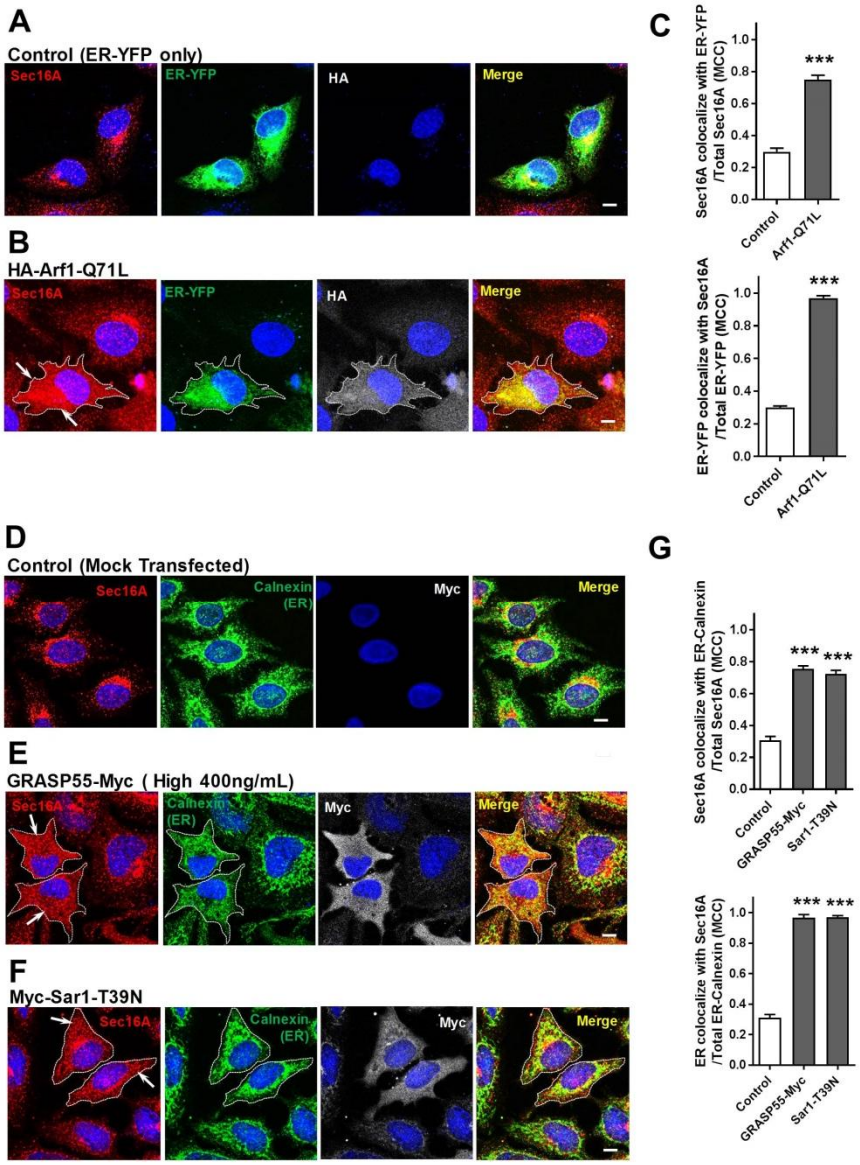

Figure 14. Sec16A relocalized within the ER region during the unconventional secretion. (A-B) Representative immunofluorescence images showed cellular distribution of Sec16A. HeLa cells were transfected with plasmids encoding the ER marker protein ER-yellow fluorescent protein (ER-YFP) with **(B)** or without **(A)** Arf1-Q71L. **(C)** Quantification results of the multiple experiments are summarized. Arf1-Q71L induced ER-to-Golgi blockade increased the percentage of ER overlapping with Sec16A (~85%) in contrast to that in control conditions (~30%). A high percentage of Sec16A colocalizes with ER-YFP (~85%) in all conditions, and analyses using Manders' colocalization coefficient

(MCC) show that ER-to-Golgi blockade increased the extent of correlation coefficient between ER-YFP and Sec16A. The MCC value calculating the fraction of Sec16A in compartments containing ER-YFP was increased to 0.75 in ER-to-Golgi blockade condition relative to that in control conditions (MCC = 0.30). The MCC value calculating the fraction of ER-YFP in compartments containing Sec16A was increased to 0.97 relative to that in control conditions (MCC = 0.30). (**D-F**) Representative immunofluorescence images showed the cellular distribution of Sec16A. Cells were transfected with mock (**D**), GRASP55-Myc (**E**), or Myc-Sar1-T39N plasmids (**F**), and the ER marker protein calnexin (green) was co-immunostained with Sec16A. GRASP55-Myc and Myc-Sar1-T39N (grey) were immunostained with anti-Myc antibody. White dotted line shows cell periphery of GRASP55-Myc or Sar1-T39N expressing cells. Arrows indicated the redistribution of Sec16A to entire cellular area by ER-to-Golgi blockade or GRASP55 overexpression. **(G)** Quantification results of the multiple experiments are summarized. ER-to-Golgi blockade increased the percentage of ER overlapping with Sec16A (~85%) relative to that in control conditions (~25%). A high percentage of Sec16A colocalizes with calnexin (~75%) in all conditions, and the MCC analyses show that ER-to-Golgi blockade and GRASP55 overexpression increased the extent of correlation coefficient between calnexin and Sec16A. The MCC value calculating the fraction of Sec16A in compartments containing calnexin was increased to 0.75 in GRASP55 overexpressed condition and to 0.72 in ER-to-Golgi blockade condition, respectively, relative to that in control conditions (MCC = 0.31). The MCC value calculating the fraction of calnexin in compartments containing Sec16A was increased to 0.97 in GRASP55 overexpressed condition and to 0.97 in ER-to-Golgi blockade condition, respectively, relative to that in control conditions (MCC = 0.31). Data shown are mean ± SEM (n = 7, each comprising analyses of 5–10 cells). Scale bar: 10 μm. ***$p < 0.001$: difference from each control. See Table 1-2 for sample size, replication and statistical information.

4. Sec16A relocalization is independent of COPII in response to ER-to-Golgi blockade and GRASP55 overexpression

To strengthen the evidence that GRASP-overexpression and ER-to-Golgi blockade specifically alternate the distribution of Sec16A, we took a more detailed approach. We compared the subcellular localization of Sec31A (as a representative subunit of core COPII component) and Sec16A (as an organizer of ERES formation) in the cells expressed with GRASP55-Myc at high level and Arf1-Q71L or Sar1-T39N induced ER-to-Golgi blockade

(Figure 15A-D). In accordance with what happened in GRASP55 overexpressed cells or Arf1-Q71L expression induced ER-to-Golgi blocked cells, Sar1-T39N expression also induced Sec16A relocalized to > 90% of the whole cell area versus > 18% in the control cells (Figure 15E). Contrastively, no significant distribution alternation of Sec31A puncta was observed in GRASP55 overexpressed and ER-to-Golgi blockade induced cells compared to control cells. More interestingly, Sar1-T39N expression caused the concentration of Sec31A to the negative end of microtubule where is also named as microtubule-organizing center (MTOC). The co-immunostaining of Sec31A and γ-tubulin which is utilized as MTOC marker was performed to verify the localization of Sec31A, (Figure 16A, B). Moreover, the cellular localization of other COPII components including Sec24B and Sec24D was also observed in control cells and in the cells expressing Arf1-Q71L (Figure 17A-D). Similar to that of Sec31A, the localization of Sec24 was not affected by ER-to-Golgi blockade (Figure 17E). Collectively, these observations suggest that the formation of GRASP-mediated unconventional secretion vesicles is supported by the ERES regulator protein Sec16A but is independent of the core COPII components.

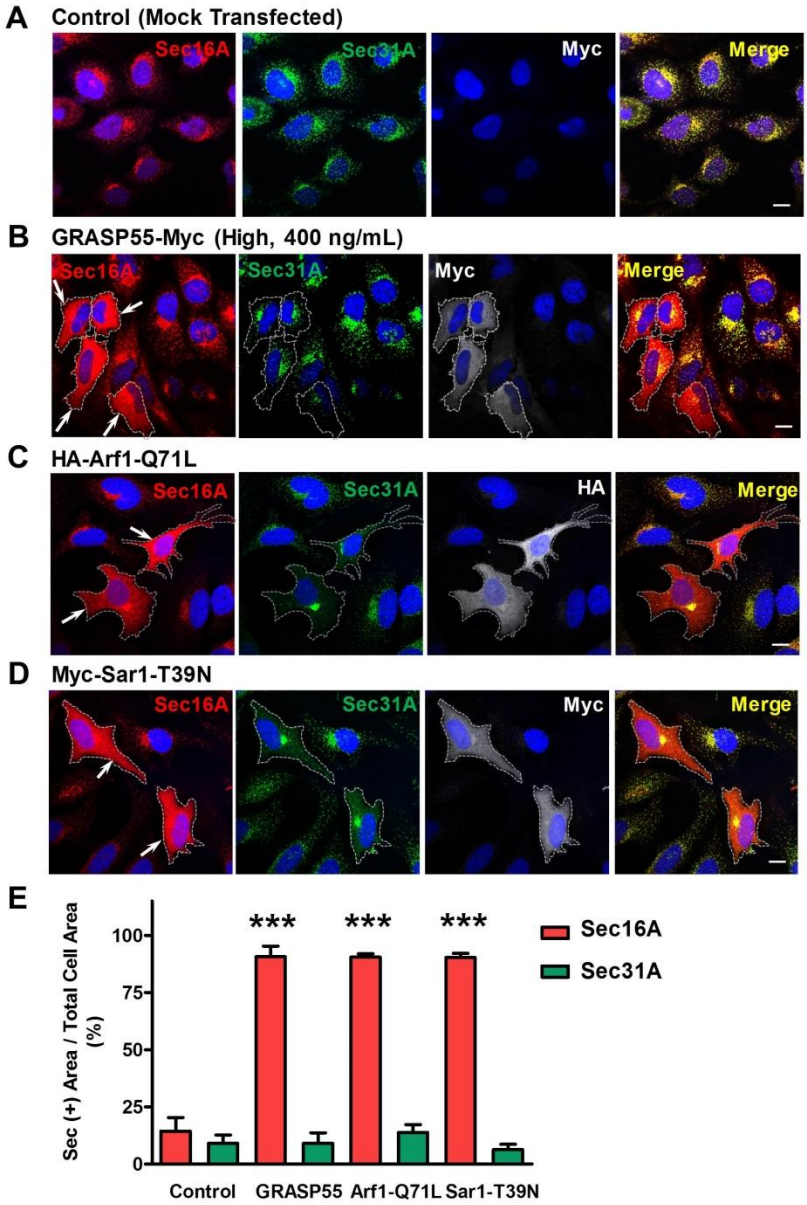

Figure 15. Sec16A but not Sec31A relocalizes when ER-to-Golgi was block or GRASP55 was overxpressed. (A-D) Intracellular distribution of Sec16A and the representative core COPII component Sec31A was compared. The cells were fixed after 24 hr and then were immunostained with anti-Sec16A and anti-Sec31A antibodies. The unconventional conditions including expression of GRASP55-Myc **(B)**, HA-Arf1-Q71L **(C)** and Myc-Sar1-T39N **(D)** were immunolabeled with anti-myc or anti-HA antibodies. Sec16A dispersed to the periphery of the cells (arrows) but localization of Sec31A was not

altered in the cells overexpressed with GRASP55 or Arf1-Q71L or Sar1-T39N (were labeled with white dotted line to compare with the control cells in each view of images). **(E)** Quantification results of the ratio of Sec16A (+) area or Sec31A (+) area versus the total cell are summarized (mean ± SEM, n ≥ 5, each comprising analyses of 5–10 cells). Morphometric analysis was performed by MetaMorph software and at least 5 cells were analyzed for each condition. Scale bar: 10 μm, ***$p < 0.001$, difference from control cells. See Table 1-2 for sample size, replication and statistical information.

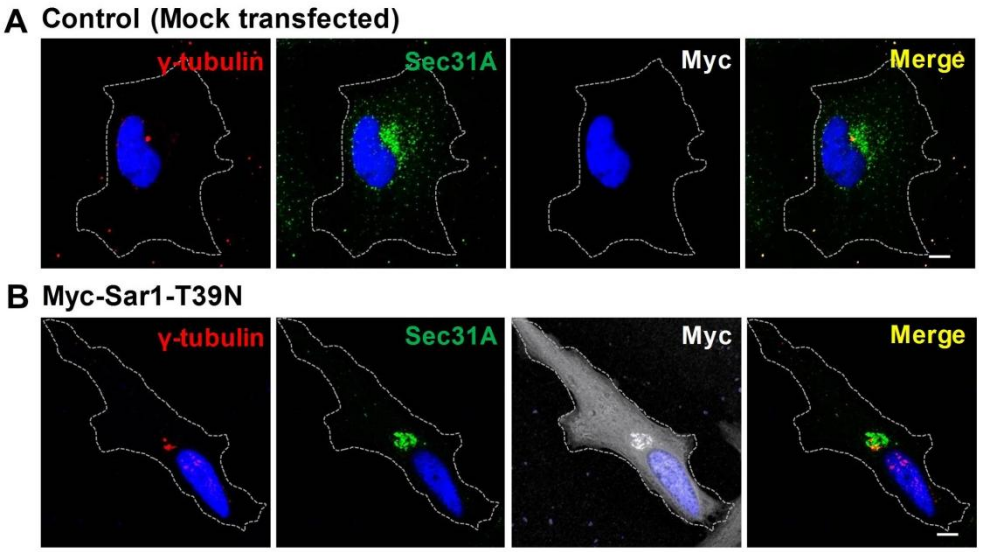

Figure 16. Sec31A concentrated near the MTOC during ER-to-Golgi blockade. The core COPII protein Sec31A and γ-tubulin were co-stained in control cells **(A)** and in the cells expressed with Sar1-T39N to induce ER-to-Golgi blockade **(B)**. γ-tubulin is a marker of microtubule-organizing center (MTOC). Sec31A was concentrated near the MTOC in cells with ER-to-Golgi blockade. Scale bar: 5 μm.

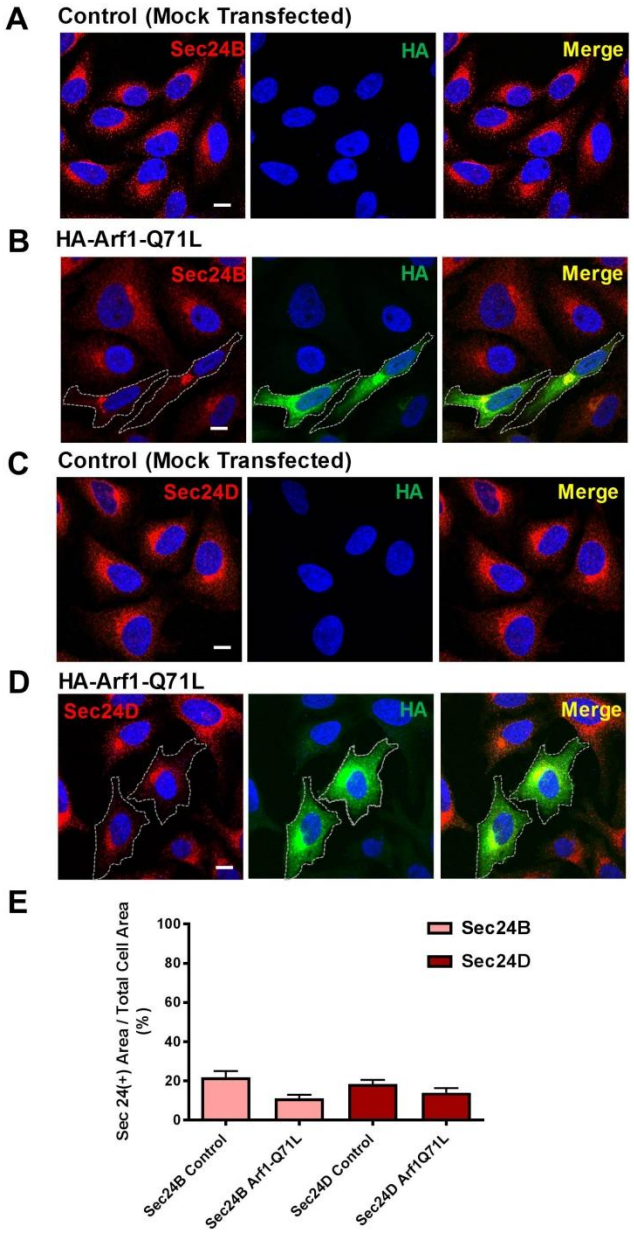

Figure 17. ER-to-Golgi blockade does not relocalize Sec24B or Sec24D. (A-D) The cellular localization of core COPII components Sec24B and Sec24D was confirmed in control cells and in cells treated with Arf1-Q71L. **(E)** Quantification of the ratio of the Sec24B (+) or Sec24D (+) area versus the total cell area in multiple experiments (mean ± SEM, n ≥ 5, each comprising analyses of 5–10 cells) are summarized. Arf1-Q71L induced ER-to-Golgi blockade has no significant effect on the localization of COPII components. Scale bar: 10 μm. See Table 1-2 for sample size, replication and statistical information.

5. IRE1α regulates the unconventional ΔF508-CFTR secretion by modulating Sec16A

To investigate the underlying machinery that Sec16A plays a scaffolding role on unconventional secretion, we studied whether there are any upstream signaling manipulating Sec16A to facilitate GRASP55 rescue the ΔF508-CFTR. According to the previous findings, IRE1α-mediated signaling, which is a key regulator of UPR, has been identified to be required for ER stress-mediated and GRASP-mediated unconventional secretion of ΔF508-CFTR.[10] In order to relieve the protein burden in the ER, IRE1-dependet UPR could also be triggered through chronic cargo overload which resulted in neo-generation of Sec16A and increment of ERES number.[31] IRE1α depletion led to abolishment of ER stress-mediated surface expression of ΔF508-CFTR. Interestingly, supplementation of Sec16A by exogenous transfection could rescue the mutant ΔF508-CFTR to the cell surface (Figure 18A, B). In accordance with the ER stress-mediated rescue results, GRASP55 overexpression induced rescue of ΔF508-CFTR was also inhibited by IRE1α silencing and was also recovered by replenishment of Sec16A (Figure 18C, D). Immunocytochemistry results further supported the notion that IRE1 is the upstream signal switches Sec16A expression and localization in "Unconventional secretion" situations (Figure 19A-D). Sec16A expression level was reduced in HeLa cells and the dispersion ratio of Sec16A in response to Arf1-Q71L induced ER-to-Golgi blockade or GRASP55 overexpression was diminished from 91% to 19% when IRE1α was depleted by siRNA (Figure 19E). Taken together, these results supply a logical clue for illustrating IRE1α-signaling is a necessary and sufficient condition for *de novo* synthesis of Sec16A during the unconventional secretion of ΔF508-CFTR.

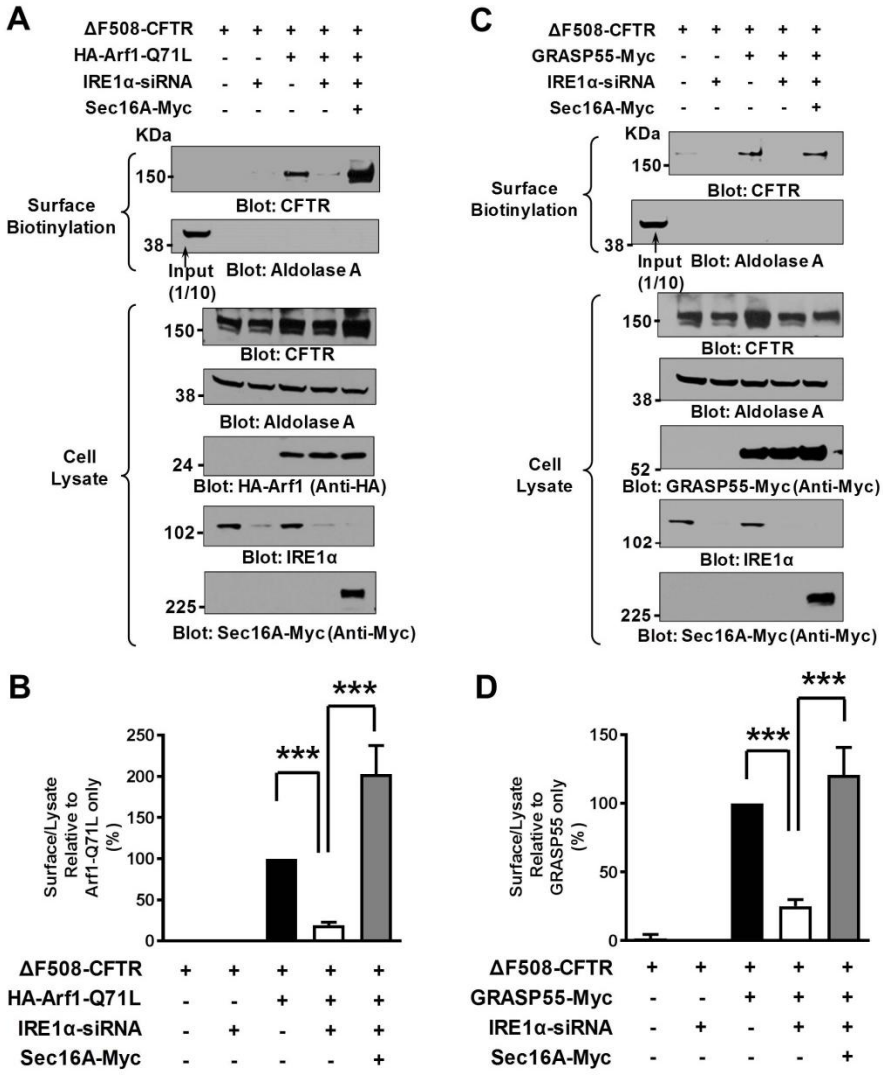

Figure 18. IRE1α-depletion inhibits the unconventional secretion of ΔF508-CFTR by down-regulating Sec16A. **(A-D)** IRE1 knock-down abolished surface rescue of ΔF508-CFTR could be recovered by Sec16A overexpression. Arf1-Q71L induced **(A)** or GRASP55-mediated **(C)** surface expression of ΔF508-CFTR was examined in the cells pre-transfected with scrambled or IRE1α-specific siRNA. IRE1α depletion abolished the surface expression of ΔF508-CFTR. Supplementation of exogenous Sec16A recovered the surface expression of ΔF508-CFTR which were inhibited by IRE1α depletion. Quantification of results of multiple experiments (mean ±SEM, n=3 ***$p < 0.001$) are summarized **(B, D).** See Table 1-2 for sample size, replication and statistical information.

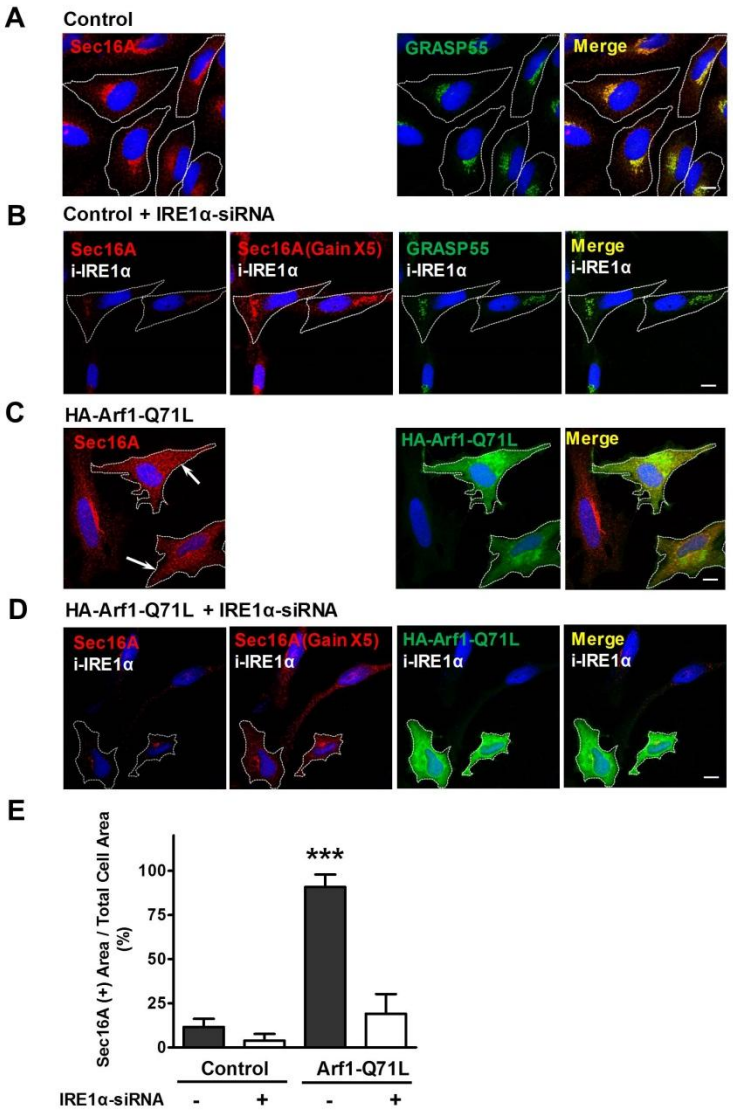

Figure 19. IRE1α depletion inhibited the redistribution of Sec16A. (A-D) Relocalization of Sec16A in cells overexpressed with GRASP55 or Arf1-Q71L were down-regulated by silencing of IRE1α. Cells overexpressed with GRASP55 or Arf1-Q71L were labeled with white dotted line. Sec16A dispersed to periphery of the cells (arrows) in the cells overexpressed with GRASP55-Myc or Arf1-Q71L. Dispersion of Sec16A in response to unconventional secretion stimuli was abolished by silencing of IRE1α. **(E)** Sec16A dispersion level was quantified as percentage of Sec16A (+) area versus total cell area. Results of multiple experiments (mean ±SEM, n ≥ 5, each comprising analyses of 5–10 cells ***$p < 0.001$) were summarized. Scale bar: 10 μm. See Table 1-2 for sample size, replication and statistical information.

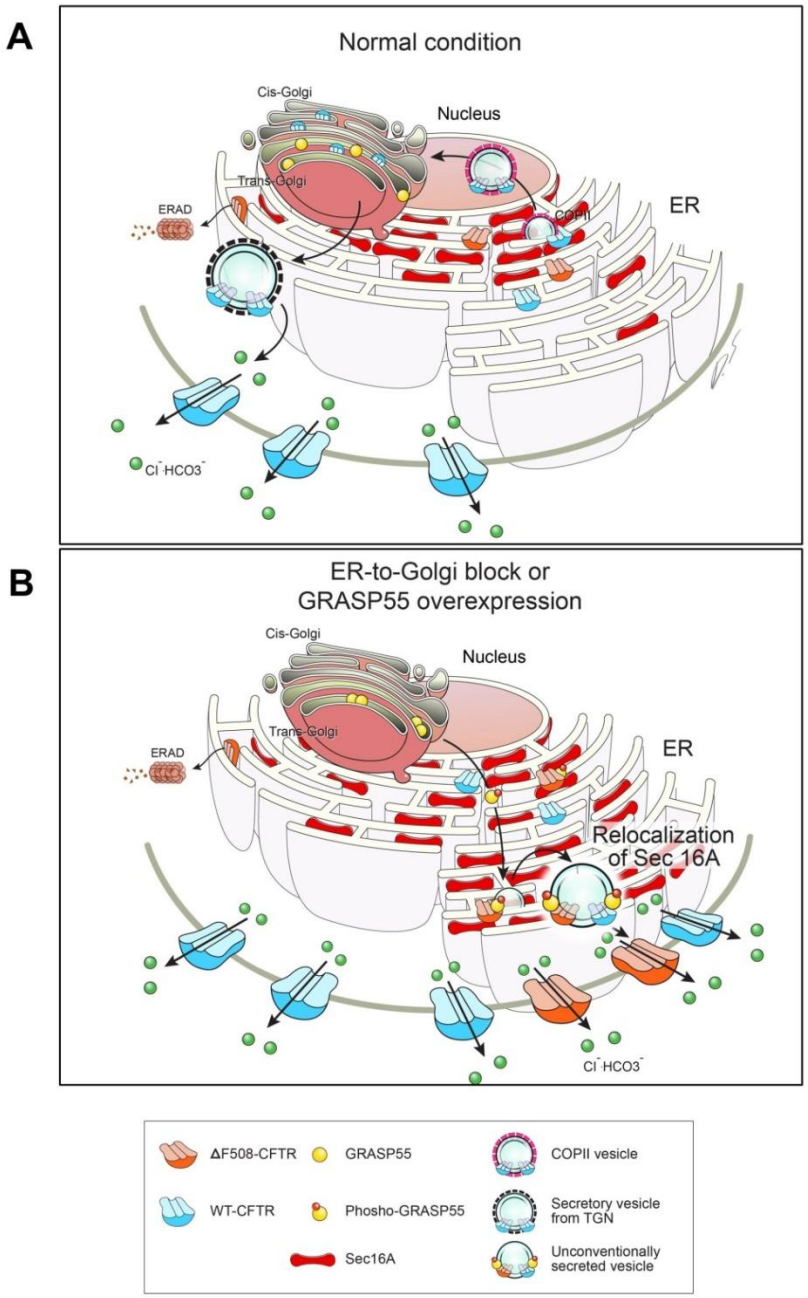

Figure 20. The graphical summary of Sec16A-facilated conventional and unconventional secretion of CFTR. Sec16A is stably associated with the ER exit sites (ERES) and acts as the scaffold for both COPII-mediated conventional secretion of CFTR and COPII-independent unconventional secretion of CFTR. Sec16A does not dissociate from ERES during the entire process in both of the mechanisms. **(A)** Under normal conditions, Sec16A localizes at the perinuclear ERES

and mediate the assembly and budding of the COPII-coated vesicles, which contains the wild-type CFTR but not ΔF508-CFTR. Wild-type CFTR exports from ER to Golgi and then passes through the Trans-Golgi-network (TGN), lastly transports to the cell surface. The ΔF508-CFTR which has folding defects would be completely degraded by ER associated degradation pathway (ERAD) and failed to reach the cell surface. **(B)** Once the ER-to-Golgi blockade or GRASP55 overexpression induced to the cell, Sec16A relocalizes from perinuclear ERES to peripheral ERES, where is adjacent to the cell surface. During this period, phosphorylated GRASP55 relocalizes from Golgi to ER and associates with Sec16A at ERES nearby the cell periphery. Core-glycosylated ΔF508-CFTR could be brought to newly established ERES and escapes from ER, and unconventionally secretes to the cell surface without passing through the Golgi complex.

Table 1. The sample size estimation and replication information, by figure

Figure number	n	
	Exact value	Paragraph
1B	WT-CFTR(4),Sec16A-siRNA treated WT-CFTR (4);Arf1-Q71L treated WT-CFTR(4), Arf1-Q71L and Sec16A-siRNA treated WT-CFTR(4)	Figure 1 legend
1D	ΔF508-CFTR (5), Sec16A-siRNA treated ΔF508-CFTR (5); Arf1-Q71L treated ΔF508-CFTR (5), Arf1-Q71L and Sec16A-siRNA treated ΔF508-CFTR (5)	Figure 1 legend
2C	ΔF508-CFTR expressed control (7), Arf1-Q71L treated(7); Sec16A-siRNA and Arf1-Q71L treated (7), Sec16B-siRNA and Arf1-Q71L treated (3); Sec23A-siRNA and Arf1-Q71L treated (4), Sec23B-siRNA and Arf1-Q71L treated (4); Sec24A-siRNA and Arf1-Q71L treated (4),Sec24B-siRNA and Arf1-Q71L treated (3), Sec24C-siRNA and Arf1-Q71L treated(3), Sec24D-siRNA and Arf1-Q71L treated (3); Sec13-siRNA and Arf1-Q71L treated (3); Sec31A-siRNA and Arf1-Q71L treated (3), Sec31B-siRNA and Arf1-Q71L treated (3)	Figure 2 legend
2E	ΔF508-CFTR expressed control (5), Arf1-Q71L treated(5); Sec16A and Sec16B-siRNAs treated (3); Sec23A and Sec23B-siRNAs and Arf1-Q71L treated (5); Sec24A, Sec24B, Sec24C and Sec24D-siRNAs and Arf1-Q71L treated (5); Sec31A and Sec31B-siRNAs and Arf1-Q71L treated(5)	Figure 2 legend
3A	Scrambled siRNA treated (3) and Sec16A-siRNA treated (3)	Figure 3 legend
3B	Scrambled siRNA treated (3) and Sec31A-siRNA treated (3)	Figure 3 legend
3C	Scrambled siRNA treated (3), Sec16A-siRNA (3), Sec16B-siRNA (3),Sec23A-siRNA (3),Sec23B-siRNA (3),Sec24A-siRNA (3),Sec24B-siRNA (3),Sec24C-siRNA (3),Sec24D-siRNA (3),Sec13-siRNA (3), Sec31A-siRNA (3), Sec31B-siRNA (3)	Figure 3 legend
4D	WT-CFTR(3),WT-CFTR 37°C 0min (3), WT-CFTR 37°C 15min (3), WT-CFTR 37°C 30min (3), WT-CFTR 37°C 60min (3); Dynasore treated WT-CFTR(3), Dynasore treated WT-CFTR(3), Dynasore treated WT-CFTR 37°C 0min (3), Dynasore treated WT-CFTR 37°C 15min (3), Dynasore treated WT-CFTR 37°C 60min (3); Dynamin-K44A treated WT-CFTR(3), Dynamin-K44A treated WT-CFTR(3), Dynamin-K44A treated WT-CFTR 37°C 0min (3), Dynamin-K44A treated WT-CFTR 37°C 15min (3), Dynamin-K44A treated WT-CFTR 37°C 60min (3)	Figure 4 legend
5A	Myc-Transferrin receptor expressed control (3), dynasore treated (3) and dynamin2-K44A treated (3)	Figure 5 legend

5B	WT-CFTR expressed control (6),dynasore treated (6), Arf1-Q71L treated (6), dynasore and Arf1-Q71L treated (6)	Figure 5 legend
5C	ΔF508-CFTR expressed control (6), dynasore treated (6), Arf1-Q71L treated (6), dynasore and Arf1-Q71L treated (6)	Figure 5 legend
5D	ΔF508-CFTR expressed control (4), dynamin2-K44A treated (4), Arf1-Q71L treated (4), dynamin2-K44A and Arf1-Q71L treated (4)	Figure 5 legend
6E	WT-CFTR expressed control (25), ΔF508-CFTR (25), Sar1-T39N treated ΔF508-CFTR (30), Sec16A-siRNA and Sar1-T39N treated ΔF508-CFTR (30)	Figure 6 legend
7B	ΔF508-CFTR expressed control (3); Myc-GRASP55, GRASP55-Myc, GRASP55 treated (3); Sec16A-siRNA and Myc-GRASP55, GRASP55-Myc, GRASP55 treated (3)	Figure 7 legend
8B	Control(3), Arf1-Q71L treated (3)	Figure 8 legend
9E	perinuclear (5) and peripheral (5) repectively in Control, Thapsigargin treated, Arf1-Q71L treated, Sar1-T39N treated conditions	Figure 9 legend
11D	Control (5); Arf1-Q71L treated (5)	Figure 10 legend
12D	Control (5); GRASP55-Myc(low) (5); GRASP55-Myc (high) (5)	Figure 12 legend
14C	Control (7), Arf1-Q71L treated (7)	Figure 14 legend
14G	Control (7), GRASP55-Myc treated (7), Sar1-T39N treated (7)	Figure 14 legend
15E	Control Sec16A and Sec31A(9); GRASP55 overepxressed Sec16A (10) and Sec31A (10); Arf1-Q71L treated Sec16A(10), Arf1-Q71L treated Sec16A(10), Sar1-T39N treated Sec31A (5) and Sec31A (5),	Figure 15 legend
17E	Control Se24B (7), Arf1-Q71L treated Sec24B; Control Se24D (10), Arf1-Q71L treated Sec24D(10);	Figure 17 legend
18B	ΔF508-CFTR expressed control (3);IRE1α-siRNA treated (3); Arf1-Q71L treated (3); IRE1α-siRNA,Arf1-Q71L treated (3); Sec16A overepxressed and IRE1α-siRNA,Arf1-Q71L treated	Figure 18 legend
18D	ΔF508-CFTR expressed control (3);IRE1α-siRNA treated (3); GRASP55-Myc treated (3); IRE1α-siRNA,GRASP55-Myc treated (3); Sec16A overepxressed and IRE1α-siRNA,GRASP55-Myc treated (3)	Figure 18 legend
19E	Control (5), IRE1α-siRNA (5); Arf1-Q71L treated (9), Arf1-Q71L and IRE1α-siRNA treated (8)	Figure 19 legend

Table 2. The statistical information reporting, by figure

Figure number	Descriptive states (Average)	Statistical test					
		Which test	Exact value of N	Definition of center	Exact p-values	Multiple test correction	Paragraph
1B	error bars are mean ± SEM	Paired t-test	3	band C: WT-CFTR;	Surface expression of WT-CFTR band C: control vs Sec16A-siRNA p=0.0273	Dunnett's Multiple Comparison Test	Figure 1 legend
			4	band B: Arf1 treated WT-CFTR	Surface expression of Arf1-Q71L treated band B of WT-CFTR: control vs Sec16A-siRNA treated p=0.0005		
1D		One-way ANOVA	5	Arf1-Q71L treated ΔF508-CFTR	Surface expression of Arf1-Q71L treated ΔF508-CFTR ANOVA summary: p< 0.0001; Dunnett's Multiple Comparison Test: ΔF508-CFTR vs ΔF508-CFTR+ Arf1-Q71L p< 0.001; ΔF508-CFTR+Arf1-Q71L vs ΔF508-CFTR+Arf1-Q71L+Sec16A-siRNA p< 0.001		
2C			3~7	Arf1-Q71L treated ΔF508-CFTR	Surface expression of Arf1 treated ΔF508-CFTR ANOVA summary: p< 0.0001; Dunnett's Multiple Comparison Test: ΔF508-CFTR vs ΔF508-CFTR+ Arf1-Q71L p<0.0001; ΔF508-CFTR+ Arf1-Q71L vs ΔF508-CFTR+Arf1Q71L+Sec16A-siRNA p< 0.001		Figure 2legend

2E	error bars are mean ± SEM	One-way ANOVA	5	Arf1-Q71L treated ΔF508-CFTR	Surface expression of Arf1 treated ΔF508-CFTR ANOVA summary: p< 0.0001; Dunnett's Multiple Comparison Test: ΔF508-CFTR vs ΔF508-CFTR+Arf1-Q71L p< 0.0001; ΔF508-CFTR+Arf1-Q71L vs ΔF508-CFTR+Arf1-Q71L+Sec16A+B-siRNA p< 0.0001; ΔF508-CFTR+Arf1-Q71L vs ΔF508-CFTR+ Arf1-Q71L+Sec23A+B-siRNA n.s. ; ΔF508-CFTR+Arf1-Q71L vs ΔF508-CFTR+Arf1-Q71L+Sec24A+B+C+D-siRNA n.s. ; ΔF508-CFTR+Arf1-Q71L vs ΔF508-CFTR+Arf1-Q71L+Sec31A+B-siRNA n.s.	Dunnett's Multiple Comparison Test	Figure 2legend
3A		Paired t-test	3	Scrambled siRNA treated	Protein expression of Sec16A: Control vs Sec16A-siRNA treated p=0.0055		Figure 3 legend
3B			3	Scrambled siRNA treated	Protein expression of Sec31A: Control vs Sec31A-siRNA treated p=0.0003		

3C	error bars are mean ± SEM	One-way ANOVA	3	Scrambled siRNA treated	mRNA expression ANOVA summary: p< 0.0001; Dunnett's Multiple Comparison Test: control vs Sec16A-siRNA treated p< 0.0001; control vs Sec16B-siRNA p< 0.0001; control vs Sec23A-siRNA p< 0.0001; control vs Sec23B-siRNA p<0.0001;control vs Sec24A-siRNA p< 0.0001; control vs Sec24B-siRNA p< 0.0001; control vs Sec24C-siRNA p< 0.0001; control vs Sec24D-siRNA p< 0.0001; control vs Sec13-siRNA p< 0.0001; control vs Sec31A-siRNA p< 0.0001; control vs Sec31B-siRNA p< 0.0001	Dunnett's Multiple Comparison Test	Figure 3 legend
3D			3	Scrambled siRNA treated	mRNA expression ANOVA summary: p< 0.0001; Dunnett's Multiple Comparison Test: control vs Sec16A-siRNA treated p< 0.0001; control vs Sec16B-siRNA p< 0.0001;		
3E			3	Scrambled siRNA treated	mRNA expression ANOVA summary: p< 0.0001; Dunnett's Multiple Comparison Test: control vs Sec23A-siRNA treated p< 0.0001; control vs Sec13B-siRNA p< 0.0001.		
3F			3	Scrambled siRNA treated	mRNA expression ANOVA summary: p< 0.0001; Dunnett's Multiple Comparison Test: control vs Sec24A-siRNA treated p< 0.0001; control vs Sec24B-siRNA p< 0.0001; control vs Sec24C-siRNA p<0.0001; control vs Sec24D-siRNA p< 0.0001.		

3G			3	Scrambled siRNA treated	mRNA expression ANOVA summary: p< 0.0001; Dunnett's Multiple Comparison Test: control vs Sec31A-siRNA treated p< 0.0001; control vs Sec31B-siRNA p< 0.0001.		Figure 3 legend
4D	error bars are mean ± SEM	One-way ANOVA	3	WT-CFTR	Internalized CFTR(0min) ANOVA summary: p=0.1116; Dunnett's Multiple Comparison Test: 0 min CFTR vs CFTR+Dynasore n.s.; 0 min CFTR vs CFTR+Dynamin-K44A n.s.; Internalized CFTR(15min) ANOVA summary: p=0.0001; Dunnett's Multiple Comparison Test: 15min CFTR vs CFTR+Dynasore p< 0.001; 15min CFTR vs CFTR+Dynamin-K44A p< 0.001; Internalized CFTR(30min) ANOVA summary: p< 0.01; Dunnett's Multiple Comparison Test: 30min CFTR vs CFTR+Dynasore p< 0.01; 30min CFTR vs CFTR+Dynamin-K44A p< 0.05; Internalized CFTR(60min) ANOVA summary: p< 0.0001; Dunnett's Multiple Comparison Test: 60min CFTR vs CFTR+Dynasore p< 0.0001; 60min CFTR vs CFTR+Dynamin-K44A p< 0.0001	Dunnett's Multiple Comparison Test	Figure 4 legend

5A		One-way ANOVA	3	Transferrin receptor only	Surface expression of TFRC Rc ANOVA summary: p=0.0003; Dunnett's Multiple Comparison Test: control vs dyasore treated p<0.01; control vs dynamin2-K44A treated p<0.001	Dunnett's Multiple Comparison Test	Figure 5 legend
5B	error bars are mean ± SEM	Paired t-test	6	untreated WT-CFTR (band C)	Surface expression of CFTR band C: control vs dynasore treated p=0.0017		
				Arf1-Q71L treated WT-CFTR (band B)	Surface expression of CFTR band B: control vs dynasore treated p=0.7561		
5C		One-way ANOVA	6	Arf1-Q71L treated ΔF508-CFTR	Surface expression of ΔF508-CFTR ANOVA summary: not significant	Dunnett's Multiple Comparison Test	
5D			4	Arf1-Q71L treated ΔF508-CFTR	Surface expression of ΔF508-CFTR ANOVA summary: not significant		
6E	error bars are mean ± SEM	One-way ANOVA		WT-CFTR	Surface CFTR fluorescence intensity ANOVA summary: p< 0.0001; Dunnett's Multiple Comparison Test: WT-CFTR vs ΔF508-CFTR p< 0.001; WT-CFTR vs Sar1-T39N treated ΔF508-CFTR p< 0.05; WT-CFTR vs Sar1-T39N and Sec16A siRNA treated ΔF508-CFTR p< 0.01.	Dunnett's Multiple Comparison Test	Figure 6 legend

7B	error bars are mean ± SEM	Paired t-test	3	Myc-GRASP 55 treated ΔF508-CFTR	Surface expression Control vs Sec16A depleted: p=0.0035		Figure 7 legend
				GRASP 55-Myc treated ΔF 508-CFTR	Surface expression: Control vs Sec16A depleted p=0.0019		
				GRASP 55 treated ΔF508-CFTR	Surface expression: Control vs Sec16A depleted p=0.0088		
8B			3	Sec16A and GRASP 55 coexpressed	IP fold change: control vs Arf1-Q71L treated p=0.0074		Figure 8 legend
9E	error bars are mean ± SEM	One-way ANOVA	5	Perinuclear of untreated cell	Perinuclear colocalization(%) ANOVA summary: p< 0.0001; Dunnett's Multiple Comparison Test: control vs thapsigargin treated p< 0.001; control vs Arf1-Q71L treated p< 0.0001; control vs Sar1-T39N treated p< 0.0001	Dunnett's Multiple Comparison Test	Figure 9 legend
				Perpheral of untreated cell	Peripheral colocalization(%) ANOVA summary: p< 0.0001; Dunnett's Multiple Comparison Test: control vs thapsigargin treated p< 0.05; control vs Arf1-Q71L treated p< 0.001; control vs Sar1-T39N treated p< 0.0001		

11 D		Paired t-test	5	Untreated cell	Sec16A(+)/Total cell area(%): control vs Arf1-Q71L treated cell p< 0.0001		Figure 11 legend
12 D	error bars are mean ± SEM	One-way ANOVA	5	Untreated cell	Sec16A(+)/Total cell area(%) ANOVA summary: p< 0.0001; Dunnett's Multiple Comparison Test control vs GRASP55-Myc(low) n.s.; control vs GRASP55-Myc(high) p< 0.0001	Dunnett's Multiple Comparison Test	Figure 12 legend
14 C		Paired t-test	6	Untreated cell	Sec16A colocalize with ER-YFP/Total Sec16A(MCC): control vs Arf1-Q71L: p< 0.0001	Dunnett's Multiple Comparison Test	Figure 14 legend
					ER-YFP colocalize with Sec16A/Total ER-YFP(MCC): control vs Arf1-Q71L: p< 0.0001		
14 G	error bars are mean ± SEM	One-way ANOVA	6	Untreated cell	Sec16A colocalize with ER-Calnexin/Total Sec16A(MCC) ANOVA summary: p< 0.0001; Dunnett's Multiple Comparison Test control vs GRASP55-Myc: p< 0.0001; control vs Sar1-T39N: p< 0.0001;	Dunnett's Multiple Comparison Test	Figure 14 legend
					ER-Calnexin colocalize with Sec16A /Total ER-Calnexin (MCC) ANOVA summary: p< 0.0001 Dunnett's Multiple Comparison Test control vs GRASP55-Myc: p< 0.0001; control vs Sar1-T39N: p< 0.0001;		

15 E		One-way ANOVA	5~9	Untreated cell	Sec16A(+)/Total cell area(%) ANOVA summary: p< 0.0001; Dunnett's Multiple Comparison Test: control vs GRASP55 treated p< 0.001; control vs Sar1-T39N treated p< 0.001 Sec31A(+)/Total cell area(%) ANOVA summary: p value n.s.	Figure 15 legend
17 E	error bars are mean ± SEM	Paired t-test	5	Untreated cell	Sec24B(+)/Total cell area(%): control vs Arf1-Q71L: n.s.	
					Sec24D(+)/Total cell area(%): control vs Arf1-Q71L: n.s.	Figure 17 legend
18 B		One-way ANOVA	3	IRE1 depleted, Arf1-Q71L treated ΔF508-CFTR	Surface expression of ΔF508-CFTR ANOVA summary: p< 0.0001; Dunnett's Multiple Comparison Test: ΔF508-CFTR+Arf1 vs ΔF508-CFTR+ Arf1+IRE1-siRNA treated p<0.001; ΔF508-CFTR+Arf1+IRE1-siRNA vs ΔF508-CFTR+Arf1+IRE1-siRNA+Sec16A-Myc p<0.001	Figure 18 legend

18 D	error bars are mean ± SEM	One-way ANOVA	3	IRE1 depleted, GRASP55 treated ΔF508-CFTR	Surface expression of ΔF508-CFTR ANOVA summary: p< 0.0001; Dunnett's Multiple Comparison Test: ΔF508-CFTR+GRASP55 vs ΔF508-CFTR+ GRASP55+ IRE1-siRNA treated p<0.001; ΔF508-CFTR +GRASP55+IRE1-siRNA vs ΔF508-CFTR+GRASP55+IRE1-siRNA+Sec16A-Myc p<0.001	
19 E			5~8	Untreated cell	Sec16A(+)/Total cell area ANOVA summary: p< 0.0001; Dunnett's Multiple Comparison Test: control vs Arf1Q71L treated p< 0.001; control vs Arf1Q71L+IRE1-siRNA treated n.s.	Figure 19 legend

IV. DISCUSSION

Most of the secretory proteins exit the ER through cargo sorting and COPII-coated vesicles form at the specific locations on the ER membrane called ER exit sites (EREs) [22,47], consequently target to various intracellular destinations including Golgi complex, endosomes, lysosomes and the plasma membrane. In recent years, the process named unconventional secretory pathway is revealed to facilitate proteins secrete from ER and directly sort to the cell surface without entering Golgi-mediated conventional secretory pathway.[10,19,48] In current study, we demonstrate the function of ER exit sites in initiation of unconventional secretion and the scaffolding role of Sec16A that regulates the formation of GRASP-mediated tethering of cargo proteins through interacting with GRASPs. This interaction could be promoted by ER-to-Golgi blockade which induces the relocalization of GRASPs from Golgi to ERES. Additionally, upregulation of GRASPs alone attributes to localization change of GRASPs accompanying with Sec16A, which provides more opportunity for their interaction. A loss of Sec16A abolishes both COPII-dependent secretion of wild-type CFTR and COPII-independent unconventional secretion of mutant ΔF508-CFTR. Interestingly, depletion of IRE1α also contributes to impairment of adaptive Sec16A neo-synthesis in response to ER-to-Golgi blockade or ER stress and disruption of unconventional ΔF508-CFTR secretion at ERES.

Sec16A has been identified as a characterized modulator of ERES biogenesis rather than a coat component,[26,28] making an indispensable contribution to the organization of ERES[29] and COPII-mediated ER export.[38,49] Sec16 is a large hydrophilic protein tightly associating with ERES and its localization at ERES is independent of downstream COPII components which cycle on and off the membrane during the ER-to-Golgi transport.[29] RNAi-mediated knockdown of Sec16 was previously reported to disrupt ERES and ER export of glycoprotein.[31,38] Additionally, it was identified that TFG-1 depletion leads to impairment of assembling of scaffolding protein Sec16 with COPII complexes giving rise to abolishment of ER export.[50] When the anchoring of Sec16A at the ERES was weakened by loss-of-function of Lrrk2 (Leucine-rich repeat kinase2, Parkinson's disease related gene), ER-to-Golgi export was impaired because of dysfunction of ERES.[51] In consideration of these

findings, we intuitively assume that Sec16A acts as a functional regulation factor for assembling of GRASP and misfolded proteins at the early stages of unconventional secretion.

1. **Sec16A functions as a scaffolding protein for unconventional secretion independent of COPII-related manner.**

The inhibition of conventional ER-to-Golgi secretory pathway could be induced by expression of dominant-negative form of Sar1 which is the GTPase catalysing COPII assembly or expression of dominant-negative form of Arf1 which is the GTPase catalyzing assembly of COPI components.[40,52] Extraordinarily, trafficking of CFTR could not be completely abolished but the ER core-glycosylated form could transport to the cell surface bypassing the Golgi instead.[10,41] Interestingly, in our results, both complex-glycosylated and core-glycosylated form of CFTR could not reach the cell surface following the depletion of Sec16A (Figure 1, 2, 6). Unlike Sec16A, COPII coat components are not involved in formation of GRASP-mediated unconventional secretory vesicles (Figure 2). In addition to this, the stimuli activating unconventional secretion resulted in Sec16A relocalized to the ERES nearby the cell periphery but Sec31A relocalized to the ERES adjacent to the nucleus MTOC resulting in dysfunction of ER-to-Golgi anterograde transport (Figure 15, 16). These results suggest that Sec16A takes participates in GRASP-mediated unconventional secretion no matter that COPII-mediated ER export was abolished. Taken together, the scaffolding role of Sec16A in the unconventional secretion route is independent of COPII machinery.

2. **Sec16A interacts and synchronizes its redistribution with GRASP55 during unconventional secretion.**

It is noticeable that Sec16 stabilize COPII assembly by interacting with cargo-Sec23-Sec24 to prevent premature disassembly of COPII.[27,53,54] Our previous study indicated that blockade of ER-to-Golgi route enabled the interaction between GRASP and core-glycosylated CFTR.[10] When it comes to the present study, ER-to-Golgi blockade also promoted GRASP55 to associate with Sec16A (Figure 8), suggesting that Sec16A may

recruit the Golgi localized GRASP55 onto ERES firstly and form complexes with GRASP55 containing the ΔF508-CFTR cargos under the conditions of ER-to-Golgi blockade.

GRASP65 and GRASP55 are Golgi matrix proteins attach peripherally to the cytoplasmic surface of Golgi membrane of the cis- and medial-trans cisternae, respectively.[14] Therefore, in the beginning of our study, how these Golgi-localized proteins encounter and survive the ER-localized misfolded proteins and finally facilitate them transport to the plasma membrane was the problem we focus on. Fortunately, we found the GRASPs dissociate from Golgi membrane and redistribute toward the cell periphery. It has been revealed in our recent report that the ER relocalization of GRASP55 provides a sufficient condition for unconventional secretion of CFTR.[46] It is worth pointing out that the major subcellular localization of Sec16A directs to the cell periphery altogether with GRASP55 when ER-to-Golgi transport was block (Figure 11C) which enabled the surface expression of ΔF508-CFTR (Figure 11B). We further confirmed these observations in the GRASP-overepxressed cells (Figure 12), where unconventional secretion could also be facilitated. In consistent with previous report,[10]overexpression of GRASP55 resulted in surface rescue of ΔF508-CFTR but the rescue effects was diminished by Sec16A depletion (Figure 7) indicating that GRASP-mediated unconventional secretion depends on the assistance of Sec16A. Surprisingly, low expression of exogenous GRASP could not induce the surface expression of ΔF508-CFTR (Figure 13A), moreover, low expression of GRASP55 was ineffective on Sec16A redistribution comparing to high expression of GRASP55 (Figure 12B, C). High expression of GRASP55 led to redistribution of Sec16A to the periphery of the cells and surface expression of ΔF508-CFTR (Figure 12C, D and Figure 13B), providing an evidence for illustrating the significance of relocalization of both Sec16A and GRASP55 in unconventional secretion. In a word, Sec16A regulating the initiation of unconventional secretion cooperates with GRASPs.

3. IRE1α-mediated UPR acts as upstream modulator for Sec16A in the unconventional secretion.

Another noticeable finding of our study is that the *de novo* generation of the scaffolding protein Sec16A in response to ER stress or upregulation of GRASP is regulated by IRE1α-mediated UPR. ER relieve the ER stress resulting from accumulation of unfolded proteins and by triggering UPR related signaling pathway to maintain homeostasis in the ER lumen,.[55] Generally, UPR reduces the protein load in ER by decreasing the gene transcription and translation of secretory proteins and rebalances the protein folding homeostasis by removing misfolded proteins into ERAD.[56] In our previous study, ER stress activated the cell surface targeting secretion of misfolded proteins via the unconventional route to relieve the ER burden,[10] which could also be considered as a result of UPR. IRE1α is one of ER stress sensors containing three branches of signaling activating the UPR.[32] The chronic increase of cargo load in ER triggered UPR and sequentially new ERES generated in order to enhance the secretory flux. This chronic adaption of ERES generation was identified to be dependent on IRE1α-controlled UPR.[31] Moreover, basal activity of IRE1α is also critically involved in GRASP-mediated rescue of ΔF508-CFTR.[10] Our current findings now clearly demonstrate the IRE1α -mediated UPR is the upstream signaling that regulates newly generation and anchoring of Sec16A at ERES to make preparation for GRASP-mediated unconventional secretion. Depletion of IRE1α consequently inhibited the surface expression of ΔF508-CFTR, fortunately, ΔF508-CFTR simply rescued by supplementation of Sec16A (Figure 18). In combination with the previous opinion that cargo load triggering UPR results in a strong induction of Sec16A and generation of new ERES,[31] UPR triggered by misfolded ΔF508-CFTR failed to transmit this signal through IRE1α-signaling due to IRE1α depletion. As a result, additional induction of Sec16A was abandoned and pre-existing Sec16A was insufficient to assemble ΔF508-CFTR at the ERES. These results altogether suggest that Sec16A provide more spatial opportunities for ΔF508-CFTR exit from ER during unconventional secretion and the amount of Sec16A is upregulated by IRE1α-controled UPR.

V. CONCLUSION

The misfolded mutant ΔF508-CFTR could be rescued from ER associated degradation (ERAD) and this process is dependent on GRASP mediated unconventional secretion. The current investigation shows that Sec16A, the key regulator of ER exit sites organization, is also responsible for both the conventional and unconventional secretion of CFTR. Sec16A cooperates with GRASP to assemble the vesicles containing ΔF508-CFTR when the ER-to-Golgi transport was blocked. The role of Sec16A that facilitates the unconventional secretion is due to its plus-end-toward relocalization in response to ER-to-Golgi blockade or GRASP55-overexpression. Subsequently, Sec16A provides the ΔF508-CFTR with a convenient platform near the cell periphery to escape from ER and directly transport to the cell surface. Moreover, the regulatory function of Sec16A in the unconventional secretion is modulated by IRE1α-mediated UPR.

REFERENCES

1. Cheng SH, Gregory RJ, Marshall J, Paul S, Souza DW, White GA, et al. Defective intracellular transport and processing of CFTR is the molecular basis of most cystic fibrosis. Cell 1990;63:827-34.
2. O'Riordan CR, Lachapelle AL, Marshall J, Higgins EA, Cheng SH. Characterization of the oligosaccharide structures associated with the cystic fibrosis transmembrane conductance regulator. Glycobiology 2000;10:1225-33.
3. Lukacs GL, Verkman AS. CFTR: folding, misfolding and correcting the DeltaF508 conformational defect. Trends Mol Med 2012;18:81-91.
4. Park HW, Nam JH, Kim JY, Namkung W, Yoon JS, Lee JS, et al. Dynamic regulation of CFTR bicarbonate permeability by $[Cl^-]_i$ and its role in pancreatic bicarbonate secretion. Gastroenterology 2010;139:620-31.
5. LaRusch J, Jung J, General IJ, Lewis MD, Park HW, Brand RE, et al. Mechanisms of CFTR functional variants that impair regulated bicarbonate permeation and increase risk for pancreatitis but not for cystic fibrosis. PLoS Genet 2014;10:e1004376.
6. Lee JH, Choi JH, Namkung W, Hanrahan JW, Chang J, Song SY, et al. A haplotype-based molecular analysis of CFTR mutations associated with respiratory and pancreatic diseases. Hum Mol Genet 2003;12:2321-32.
7. Riordan JR, Rommens JM, Kerem B, Alon N, Rozmahel R, Grzelczak Z, et al. Identification of the cystic fibrosis gene: cloning and characterization of complementary DNA. Science 1989;245:1066-73.
8. Ward CL, Omura S, Kopito RR. Degradation of CFTR by the ubiquitin-proteasome pathway. Cell 1995;83:121-7.
9. Namkung W, Kim KH, Lee MG. Base treatment corrects defects due to misfolding of mutant cystic fibrosis transmembrane conductance regulator. Gastroenterology 2005;129:1979-90.
10. Gee HY, Noh SH, Tang BL, Kim KH, Lee MG. Rescue of DeltaF508-CFTR trafficking via a GRASP-dependent unconventional secretion pathway. Cell 2011;146:746-60.

11. Nickel W, Seedorf M. Unconventional mechanisms of protein transport to the cell surface of eukaryotic cells. Annu Rev Cell Dev Biol 2008;24:287-308.
12. Barr FA, Puype M, Vandekerckhove J, Warren G. GRASP65, a protein involved in the stacking of Golgi cisternae. Cell 1997;91:253-62.
13. Shorter J, Watson R, Giannakou ME, Clarke M, Warren G, Barr FA. GRASP55, a second mammalian GRASP protein involved in the stacking of Golgi cisternae in a cell-free system. Embo j 1999;18:4949-60.
14. Xiang Y, Wang Y. GRASP55 and GRASP65 play complementary and essential roles in Golgi cisternal stacking. J Cell Biol 2010;188:237-51.
15. Feinstein TN, Linstedt AD. GRASP55 regulates Golgi ribbon formation. Mol Biol Cell 2008;19:2696-707.
16. Levi SK, Bhattacharyya D, Strack RL, Austin JR, 2nd, Glick BS. The yeast GRASP Grh1 colocalizes with COPII and is dispensable for organizing the secretory pathway. Traffic 2010;11:1168-79.
17. Schotman H, Karhinen L, Rabouille C. dGRASP-mediated noncanonical integrin secretion is required for Drosophila epithelial remodeling. Dev Cell 2008;14:171-82.
18. Xiang Y, Zhang X, Nix DB, Katoh T, Aoki K, Tiemeyer M, et al. Regulation of protein glycosylation and sorting by the Golgi matrix proteins GRASP55/65. Nat Commun 2013;4:1659.
19. Manjithaya R, Anjard C, Loomis WF, Subramani S. Unconventional secretion of Pichia pastoris Acb1 is dependent on GRASP protein, peroxisomal functions, and autophagosome formation. J Cell Biol 2010;188:537-46.
20. Duran JM, Anjard C, Stefan C, Loomis WF, Malhotra V. Unconventional secretion of Acb1 is mediated by autophagosomes. J Cell Biol 2010;188:527-36.
21. Bruns C, McCaffery JM, Curwin AJ, Duran JM, Malhotra V. Biogenesis of a novel compartment for autophagosome-mediated unconventional protein secretion. J Cell Biol 2011;195:979-92.
22. Bannykh SI, Rowe T, Balch WE. The organization of endoplasmic reticulum export complexes. J Cell Biol 1996;135:19-35.
23. Yoshihisa T, Barlowe C, Schekman R. Requirement for a GTPase-activating protein

in vesicle budding from the endoplasmic reticulum. Science 1993;259:1466-8.

24. Bi X, Corpina RA, Goldberg J. Structure of the Sec23/24-Sar1 pre-budding complex of the COPII vesicle coat. Nature 2002;419:271-7.
25. Stagg SM, Gurkan C, Fowler DM, LaPointe P, Foss TR, Potter CS, et al. Structure of the Sec13/31 COPII coat cage. Nature 2006;439:234-8.
26. Gimeno RE, Espenshade P, Kaiser CA. COPII coat subunit interactions: Sec24p and Sec23p bind to adjacent regions of Sec16p. Mol Biol Cell 1996;7:1815-23.
27. Supek F, Madden DT, Hamamoto S, Orci L, Schekman R. Sec16p potentiates the action of COPII proteins to bud transport vesicles. J Cell Biol 2002;158:1029-38.
28. Ivan V, de Voer G, Xanthakis D, Spoorendonk KM, Kondylis V, Rabouille C. Drosophila Sec16 mediates the biogenesis of tER sites upstream of Sar1 through an arginine-rich motif. Mol Biol Cell 2008;19:4352-65.
29. Hughes H, Budnik A, Schmidt K, Palmer KJ, Mantell J, Noakes C, et al. Organisation of human ER-exit sites: requirements for the localisation of Sec16 to transitional ER. J Cell Sci 2009;122:2924-34.
30. Farhan H, Wendeler MW, Mitrovic S, Fava E, Silberberg Y, Sharan R, et al. MAPK signaling to the early secretory pathway revealed by kinase/phosphatase functional screening. J Cell Biol 2010;189:997-1011.
31. Farhan H, Weiss M, Tani K, Kaufman RJ, Hauri HP. Adaptation of endoplasmic reticulum exit sites to acute and chronic increases in cargo load. Embo j 2008;27:2043-54.
32. Lin JH, Li H, Yasumura D, Cohen HR, Zhang C, Panning B, et al. IRE1 signaling affects cell fate during the unfolded protein response. Science 2007;318:944-9.
33. Gee HY, Tang BL, Kim KH, Lee MG. Syntaxin 16 binds to cystic fibrosis transmembrane conductance regulator and regulates its membrane trafficking in epithelial cells. J Biol Chem 2010;285:35519-27.
34. Dunn KW, Kamocka MM, McDonald JH. A practical guide to evaluating colocalization in biological microscopy. American Journal of Physiology - Cell Physiology 2011;300:C723-C42.
35. Park J, Kwak JO, Riederer B, Seidler U, Cole SP, Lee HJ, et al. Na(+)/H(+)

exchanger regulatory factor 3 is critical for multidrug resistance protein 4-mediated drug efflux in the kidney. J Am Soc Nephrol 2014;25:726-36.

36. Martinez-Menarguez JA, Prekeris R, Oorschot VM, Scheller R, Slot JW, Geuze HJ, et al. Peri-Golgi vesicles contain retrograde but not anterograde proteins consistent with the cisternal progression model of intra-Golgi transport. J Cell Biol 2001;155:1213-24.
37. Tokuyasu KT. Immunochemistry on ultrathin frozen sections. Histochem J 1980;12:381-403.
38. Bhattacharyya D, Glick BS. Two mammalian Sec16 homologues have nonredundant functions in endoplasmic reticulum (ER) export and transitional ER organization. Mol Biol Cell 2007;18:839-49.
39. Kapetanovich L, Baughman C, Lee TH. Nm23H2 facilitates coat protein complex II assembly and endoplasmic reticulum export in mammalian cells. Mol Biol Cell 2005;16:835-48.
40. Dascher C, Balch WE. Dominant inhibitory mutants of ARF1 block endoplasmic reticulum to Golgi transport and trigger disassembly of the Golgi apparatus. J Biol Chem 1994;269:1437-48.
41. Yoo JS, Moyer BD, Bannykh S, Yoo HM, Riordan JR, Balch WE. Non-conventional trafficking of the cystic fibrosis transmembrane conductance regulator through the early secretory pathway. J Biol Chem 2002;277:11401-9.
42. Glebov OO, Bright NA, Nichols BJ. Flotillin-1 defines a clathrin-independent endocytic pathway in mammalian cells. Nat Cell Biol 2006;8:46-54.
43. Damke H, Binns DD, Ueda H, Schmid SL, Baba T. Dynamin GTPase domain mutants block endocytic vesicle formation at morphologically distinct stages. Mol Biol Cell 2001;12:2578-89.
44. Kuge O, Dascher C, Orci L, Rowe T, Amherdt M, Plutner H, et al. Sar1 promotes vesicle budding from the endoplasmic reticulum but not Golgi compartments. J Cell Biol 1994;125:51-65.
45. Kondylis V, Spoorendonk KM, Rabouille C. dGRASP localization and function in the early exocytic pathway in Drosophila S2 cells. Mol Biol Cell 2005;16:4061-72.

46. Kim J, Noh SH, Piao H, Kim DH, Kim K, Cha JS, et al. Monomerization and ER Relocalization of GRASP Is a Requisite for Unconventional Secretion of CFTR. Traffic 2016;17:733-53.
47. Barlowe C, Orci L, Yeung T, Hosobuchi M, Hamamoto S, Salama N, et al. COPII: a membrane coat formed by Sec proteins that drive vesicle budding from the endoplasmic reticulum. Cell 1994;77:895-907.
48. Dupont N, Jiang S, Pilli M, Ornatowski W, Bhattacharya D, Deretic V. Autophagy-based unconventional secretory pathway for extracellular delivery of IL-1beta. Embo j 2011;30:4701-11.
49. Iinuma T, Shiga A, Nakamoto K, O'Brien MB, Aridor M, Arimitsu N, et al. Mammalian Sec16/p250 plays a role in membrane traffic from the endoplasmic reticulum. J Biol Chem 2007;282:17632-9.
50. Witte K, Schuh AL, Hegermann J, Sarkeshik A, Mayers JR, Schwarze K, et al. TFG-1 function in protein secretion and oncogenesis. Nat Cell Biol 2011;13:550-8.
51. Cho HJ, Yu J, Xie C, Rudrabhatla P, Chen X, Wu J, et al. Leucine-rich repeat kinase 2 regulates Sec16A at ER exit sites to allow ER-Golgi export. Embo j 2014;33:2314-31.
52. Russell C, Stagg SM. New insights into the structural mechanisms of the COPII coat. Traffic 2010;11:303-10.
53. Kung LF, Pagant S, Futai E, D'Arcangelo JG, Buchanan R, Dittmar JC, et al. Sec24p and Sec16p cooperate to regulate the GTP cycle of the COPII coat. Embo j 2012;31:1014-27.
54. Watson P, Townley AK, Koka P, Palmer KJ, Stephens DJ. Sec16 defines endoplasmic reticulum exit sites and is required for secretory cargo export in mammalian cells. Traffic 2006;7:1678-87.
55. Walter P, Ron D. The unfolded protein response: from stress pathway to homeostatic regulation. Science 2011;334:1081-6.
56. Smith MH, Ploegh HL, Weissman JS. Road to ruin: targeting proteins for degradation in the endoplasmic reticulum. Science 2011;334:1086-90.

Abstract (in Korean)

GRASP을 통한 비전형적 단백이동경로에서 ER exit sites의 역할

<지도교수 이 민 구>

연세대학교 대학원 의과학과

박 학

낭포성 섬유증 유발 세포막 단백질(Cystic Fibrosis Transmembrane Conductance Regulator, CFTR)은 생체 내 기도, 장, 췌장 및 외분비선 등 장기의 상피세포 선단 표면에서 염소이온 및 중탄산이온을 비롯한 음이온의 수송을 조절하는 중요한 단백질이다. CFTR 의 508번째 페닐알라닌이 소실되는 ΔF508-CFTR 돌연변이는 낭포성 섬유증(Cystic Fibrosis, CF)을 유발하는 가장 흔한 유전변이이다. 일반적인 CFTR 단백의 경우 소포체(Endoplasmic Reticulum, ER)-골지체(Golgi apparatus)간 수송을 거쳐 세포막에 도달하게 되지만 ΔF508-CFTR 돌연변이 단백의 경우 접힘 장애를 가지게 되어 소포체 품질검사를 통과하지 못하고 소포관련 분해기전(ER associated degradation, ERAD)을 통해 분해되는 것으로 알려져 있다.

소포체-골지체간의 단백질 수송을 억제하거나 소포체 스트레스를 유발할 경우 ΔF508-CFTR 돌연변이 단백이 골지체를 우회하는 비전형적 이동경로(Unconventional secretory pathway)를 통해 세포막으로 수송되어 이온수송능력이 회복되고, 이는 GRASP (Golgi reassembly stacking protein) 에

의존적이라는 것이 선행 연구에서 보고된 바 있다. 또한 소포체 스트레스를 유발하지 않더라도 GRASP 의 과발현에 의해서도 비전형적 이동경로를 통한 ΔF508-CFTR 돌연변이 단백의 수송과 기능이 회복되는 것이 세포 및 생쥐모델을 통해서 확인되었다. 그러나 현재까지 접힘 장애가 있는 ΔF508-CFTR 이 어떻게 소포체에서 떠나 비전형적 이동경로를 통하여 세포막에 도달하는 지에 대한 정확한 기전은 밝혀진 바 없다. 따라서 본 연구에서는 이러한 기전을 밝히는 것을 주요 연구 목표로 하였다.

본 연구를 통해 소포체 출구부위(ER exit sites, ERES)에 존재 하며 소포체 출구부위의 형성에 핵심적인 역할을 하는 Sec16A 라는 단백이 비전형적 단백수송의 시작단계에서도 중요한 역할을 수행함을 밝혔다. Sec16A 의 기능을 억제한 경우 CFTR 의 전형적 수송 및 비전형적 수송이 모두 봉쇄됨을 통해서 Sec16A 가 CFTR 의 전형적 수송뿐만 아니라 비전형적 수송에도 관련이 있음을 확인하였다. 특히 ΔF508-CFTR 의 비전형적 수송을 일으키는 조건에서 Sec16A 는 GRASP55와 결합하며 세포내 분포도 GRASP55와 같이 세포핵 주변 으로부터 세포막 근처로 이동한다는 것을 공초점 형광현미경을 이용한 이미지 관찰을 통하여 알 수 있었다. 이는 Sec16가 비전형적 단백수송경로에서 GRASP55와 ΔF508-CFTR 를 세포막 가까운 부위에서 새로 생성된 소포체 출구부위에서의 결합을 돕는 스캐폴드(scaffold)로서의 역할을 수행함을 시사한다. 또한, IRE1α 에 의해 매개되는 비접힘 단백질 반응(Unfolded protein response, UPR) 신호가 이러한 Sec16A 의 작용에 관여하는 상위조절 인자임을 확인하였다.

이상의 결과를 통하여 비전형적인 단백수송경로를 통한 ΔF508-CFTR 의 세포막 발현은 Sec16A 에 의존적이라는 것을 밝혔으며 이는 낭포성 섬유증, 췌장염을 비롯한 단백 접힘 이상으로부터 기인하는 여러 질환들의 치료제 개발에 있어서 새로운 대안을 제시할 것으로 기대된다.

핵심되는 말: 비전형적 단백수송, 낭포성 섬유증, GRASP, Sec16A, 소포체 출구부위

PUBLICATION LIST

1. **Piao H**, Kim J, Noh SH, Lee MG, et al. Sec16A is critical for both conventional and unconventional secretion of CFTR. Scientific Reports 2016;6. In press
2. Kim J, Noh SH, **Piao H**, Kim DH, Kim K, Cha JS, et al. Monomerization and ER Relocalization of GRASP Is a Requisite for Unconventional Secretion of CFTR. Traffic 2016;17:733-53